Anti- SARS-CoV-2 Receptor Binding Domain Antibody Evolution after mRNA Vaccination

Alice Cho[1,*], Frauke Muecksch[2,*], Dennis Schaefer-Babajew[1,*], Zijun Wang[1,*], Shlomo Finkin[1,*],Christian Gaebler[1], Victor Ramos[1], Melissa Cipolla[1], Pilar Mendoza[1], Marianna Agudelo[1], Eva Bednarski[2], Justin DaSilva[2], Irina Shimeliovich[1], Juan Dizon[1], Mridushi Daga[1], Katrina Millard[1], Martina Turroja[1], Fabian Schmidt[2], Fengwen Zhang[2], Tarek Ben Tanfous[1], Mila Jankovic[1], Thiago Y. Oliveria[1], Anna Gazumyan[1], Marina Caskey[1], Paul D. Bieniasz[2,3], Theodora Hatziioannou[2], and Michel C. Nussenzweig[1,3].

[1]Laboratory of Molecular Immunology, The Rockefeller University, New York, NY 10065, USA

[2]Laboratory of Retrovirology, The Rockefeller University, New York, NY 10065, USA

[3]Howard Hughes Medical Institute

*equal contribution

Address correspondence to: Paul D. Bieniasz pbieniasz@rockefeller.edu; Marina Caskey mcaskey@rockefeller.edu; Theodora Hatziioannou thatziio@rockefeller.edu; or Michel C. Nussenzweig nussen@rockefeller.edu

Summary

Severe acute respiratory syndrome coronavirus 2 (SARS-CoV-2) infection produces B-cell responses that continue to evolve for at least one year. During that time, memory B cells express increasingly broad and potent antibodies that are resistant to mutations found in variants of concern[1]. As a result, vaccination of coronavirus disease 2019 (COVID-19) convalescent individuals with currently available mRNA vaccines produces high levels of plasma neutralizing activity against all variants tested[1,2]. Here, we examine memory B cell evolution 5 months after vaccination with either Moderna (mRNA-1273) or Pfizer-BioNTech (BNT162b2) mRNA vaccines in a cohort of SARS-CoV-2 naïve individuals. Between prime and boost, memory B cells produce antibodies that evolve increased neutralizing activity, but there is no further increase in potency or breadth thereafter. Instead, memory B cells that emerge 5 months after vaccination of naïve individuals express antibodies that are similar to those that dominate the initial response. While individual memory antibodies selected over time by natural infection have greater potency and breadth than antibodies elicited by vaccination, the overall neutralizing potency of plasma is greater following vaccination. These results suggest that boosting vaccinated individuals with currently available mRNA vaccines will increase plasma neutralizing activity but may not produce antibodies with breadth equivalent to those obtained by vaccinating convalescent individuals.

Between January 21 and July 20, 2021, we recruited 32 volunteers with no history of prior SARS-CoV-2 infection receiving either Moderna (mRNA-1273; n=8) or Pfizer-BioNTech (BNT162b2; n=24) mRNA vaccines for sequential blood donation. Matched samples were

42 obtained at 2 or 3 time points. Individuals indicated as "prime" were sampled an average of 2.5
43 weeks after receiving their first vaccine dose. Individuals who completed their vaccination
44 regimen were sampled after an average of 1.3 months after the boost (median=35.5 days) which
45 is not statistically different from the 1.3 month sampling in our naturally infected cohort[3]
46 (median=38.5 days, p=0.21). Individuals sampled at 1.3 months were sampled again
47 approximately 5 months after the second vaccine dose. The volunteers ranged in age from 23-78
48 years (median=34.5 years), 53% were male and 47% female (for details see Methods and
49 Supplementary Tables 1 and 2).
50
51 **Plasma binding and neutralization assays**
52 Plasma IgM, IgG, and IgA responses to SARS-CoV-2 receptor binding domain (RBD) were
53 measured by enzyme linked immunosorbent assay (ELISA)[3]. As reported by others[2,4-6] there was
54 a significant increase in IgG reactivity to RBD between prime and boost ($p<0.0001$, Fig. 1a).
55 IgM and IgA titers were lower than IgG titers and remained low after the second vaccine dose
56 (Extended data Fig. 1a and b). The magnitude of the response was inversely correlated with age
57 after the prime ($r=-0.54$, $p=0.005$), but in this limited sample set the age difference was no longer
58 significant at 1.3 or 5 months after the second vaccine dose (Fig. 1b, Extended data Fig. 1c).
59 Between 1.3 and 5 months after the boost, anti-RBD titers of IgG and IgA decreased
60 significantly. IgG titers decreased by an average of 4.3-fold (range: 1.7- to 10.2-fold) and the
61 loss of activity was directly correlated to the time after vaccination ($p<0.0001$, Fig. 1a and c and
62 Extended data Fig. 1a and b).
63

64 Neutralizing activity was measured using HIV-1 pseudotyped with the SARS-CoV-2 spike[1,3,7,8].
65 Naïve individuals showed variable responses to the initial vaccine dose with a geometric mean
66 half-maximal neutralizing titer (NT_{50}) of 171 (Fig. 1d, Supplementary Table 2). The magnitude
67 of the neutralizing responses to the initial vaccine dose in naïve volunteers was inversely
68 correlated with age (r=-0.39, p=0.05, Fig. 1e). Both binding and neutralizing responses to the
69 second vaccine dose were correlated to the prime (r=0.46, p=0.02, Extended data. Fig. 1d;
70 r=0.54, p=0.003, Extended data Fig. 1e) and produced a nearly 12-fold increase in the geometric
71 mean neutralizing response that was similar in males and females and eliminated the age-related
72 difference in neutralizing activity in the individuals in this cohort (Fig. 1d, Extended data Fig. 1f
73 and Fig. 1e and Extended data Fig. 1g). 1.3 and 5 months after the boost naïve vaccinees had 4.9-
74 and 3.6 fold higher neutralizing titers than a cohort of infected individuals measured 1.3[3]- and
75 6.2[7]-months after symptom onset, respectively (p<0.0001, Fig. 1d). Neutralizing responses were
76 directly correlated to IgG anti-RBD titers (r=0.96, p<0.0001, Fig. 1f). Thus, the data obtained
77 from this cohort agree with prior observations showing a significant increase in plasma
78 neutralizing activity that are correlated with improved vaccine efficacy in naïve individuals that
79 receive the second dose of mRNA vaccine[2,6,9,10] and higher neutralizing titers in fully vaccinated
80 than infected individuals[2,6].
81
82 The 28 individuals assayed 5 months after vaccination had a 7.1-fold decrease in geometric mean
83 neutralizing titer from their 1.3-month measurement (p<0.0001, Fig. 1d), with a range of 1.4- to
84 27-fold. Neutralizing activity was inversely correlated with the time from vaccination (r=-0.82,
85 p<0.0001, Fig. 1g), and directly correlated to IgG anti-RBD binding titers when assessed 5
86 months after vaccination (Extended data. Fig. 1h). As reported by others[11], the ratio of binding to

87 neutralizing serum titers was significantly higher in vaccinated than convalescent individuals at
88 the 1.3-month time point ($p<0.0001$, Fig. 1h). However, the difference was no longer apparent at
89 the later time point (Fig. 1h).
90
91 We and others showed that the neutralizing responses elicited by mRNA vaccination are more
92 potent against the original Wuhan Hu-1 strain than for some of the currently circulating variants
93 of concern[2,12-14]. To confirm these observations, we measured the neutralizing activity of 15
94 paired plasmas from naive individuals 1.3 and 5 months after the second vaccine dose against
95 B.1.1.7 (alpha variant), B.1.351 (beta variant), B.1.526 (iota variant), P.1 (gamma variant) and
96 B.1.617.2 (delta variant). Consistent with previous reports[13,15-17] the neutralizing activity against
97 the variants was lower than against the original Wuhan Hu-1 strain (Fig. 1i, Supplementary
98 Table 3). Initial geometric mean neutralizing titers at 1.3 months against B.1.351, B.1.1.7,
99 B.1.526, P.1 and B.1.617.2 were 5.7, 1.8, 1.1, 1.4 and 2.7-fold lower than against Wuhan-Hu
100 respectively (Fig. 1i). In the months following vaccination there was a decrease in neutralizing
101 activity against Wuhan Hu-1 (R683G) and all the variants with geometric mean neutralizing
102 titers for WT, B.1.351, B.1.1.7, B.1.526, P.1 and B.1.617.2 decreasing by 2.9-, 1.8-, 2.3-, 2.9-,
103 2.4- and 2.6-fold, respectively (Fig. 1i and Supplementary Table 3).
104
105 **Monoclonal Antibodies**
106 Circulating antibodies produced by plasma cells can prevent infection if present at sufficiently
107 high concentrations at the time of exposure. In contrast, the memory B cell compartment
108 contains long lived antigen-specific B cells that mediate rapid recall responses that contribute to
109 long term protection[18]. To examine the nature of the memory compartment elicited by one or two

110 mRNA vaccine doses and its evolution after 5 months we used flow cytometry to enumerate B
111 cells expressing receptors that bind to Wuhan Hu-1 (wild type, WT) and the B.1.351
112 K417N/E484K/N501Y variant RBDs (Fig. 2a and b, and Extended data Fig. 2). Although
113 neutralizing antibodies develop to other parts of the spike (S) protein we focused on RBD
114 because it is the dominant target of the memory antibody neutralizing response[19,20]. Wuhan-Hu
115 RBD-specific memory B cells developed after the prime in all volunteers examined and their
116 numbers increased for up to 5 months after vaccination (Fig. 2a). Memory B cells binding to the
117 B.1.351 K417N/E484K/N501Y variant RBD were detectable but in lower numbers than wild
118 type RBD-binding B cells in all samples examined (Fig. 2b). Whereas IgG memory cells
119 increased after the boost, IgM-expressing memory B cells that made up 23% of the memory
120 compartment after the prime were nearly absent after boosting (Fig. 2c). Finally, circulating
121 RBD-specific plasmablasts were readily detected after the prime but were infrequent after the
122 boost (Fig. 2d, and Extended data Fig. 2d).
123
124 The memory compartment continues to evolve up to one year after natural infection with
125 selective enrichment of cells producing broad and potent neutralizing antibodies[1]. To determine
126 how the memory compartment evolves after vaccination, we obtained 2328 paired antibody
127 sequences from 11 individuals sampled at the time points described above (Fig. 2e and f,
128 Extended Data Fig 3, Supplementary Table 4). As expected *IGHV3-30* and *IGHV3-53* were
129 over-represented after the first and second vaccine dose and remained over-represented 5 months
130 after vaccination[21-23] (Extended data Fig. 4).
131

132 All individuals examined showed expanded clones of memory B cells that expressed closely
133 related *IGHV* and *IGHL* genes (Fig. 2e and f, Extended data Fig. 4). Paired prime and 1.3 month
134 post boost samples showed expanded clones of memory B cells some of which were shared
135 across plasmablasts, IgM and IgG prime, and IgG boost memory cells (Extended data Fig. 3 and
136 5). Thus, the cell fate decision controlling the germinal center versus plasmablast decision is not
137 entirely affinity dependent since cells with the same initial affinity can enter both compartments
138 to produce clonal relatives[24].
139
140 The relative fraction of memory cells found in expanded clones varied between prime and boost
141 and between individuals and decreased over time (Fig. 2e-g). Overall, clones represented 30%,
142 21%, and 9.7% of all sequences after prime, 1.3- and 5-month time points respectively (Fig. 2g).
143 Nevertheless, clones of memory B cells continued to evolve for up to 5 months in vaccinated
144 individuals as evidenced by the appearance of unique clones. Notably, unique clones appearing
145 after 1.3 and 5 months represent a greater or equal fraction of the total memory B cell pool than
146 the persisting clones (Fig. 2e-f, 16% vs 9.6% and 5.1% vs 4.7%, respectively, Extended data Fig.
147 3b). Finally, memory B cells emerging after the boost showed significantly higher levels of
148 somatic mutations than plasmablasts or memory B cells isolated after the prime, and they
149 continue to accumulate mutations up to 5 months post-boost (Fig. 2h, and Extended data Fig.
150 3d). In conclusion the memory B cell compartment continues to evolve for up to 5 months after
151 mRNA vaccination.
152
153 **Neutralizing Activity of Monoclonal Antibodies**

154 We performed ELISAs to confirm that the antibodies isolated from memory B cells bind to RBD
155 (Extended data Fig. 6). 458 antibodies were tested by ELISA including: 88 isolated after the first
156 vaccine dose; 210 isolated after the boost; and 160 isolated from individuals that had been fully
157 vaccinated 5 months earlier. Among the 458 antibodies tested 430 (94%) bound to the Wuhan
158 Hu-1 RBD indicating that the method used to isolate RBD-specific memory B cells was highly
159 efficient (Supplementary Table 5-6). The geometric mean ELISA half-maximal concentration
160 (EC_{50}) of the antibodies obtained after prime, and 1.3- and 5-months after the second dose was
161 3.5, 2.9 and 2.7 ng/ml respectively, suggesting no major change in binding over time after
162 vaccination (Extended data Fig. 6 and Supplementary Table 5-6).
163
164 430 RBD-binding antibodies were tested for neutralizing activity using HIV-1 pseudotyped with
165 the SARS-CoV-2 spike[3,8]. The geometric mean half-maximal inhibitory concentration (IC_{50}) of
166 the RBD-specific memory antibodies improved from 376 ng/ml to 153 ng/ml between the first
167 and second vaccine dose (p=0.0005, Fig. 3a). The improvement was reflected in all clones (IC_{50}
168 377 vs. 171 ng/ml, p=0.01 Fig. 3b), persisting clones (IC_{50} 311 vs. 168, Fig. 3c, Supplementary
169 Table 6), unique clones (IC_{50} 418 vs. 165 ng/ml, p=0.03 Fig. 3d), and single antibodies (IC_{50} 374
170 vs. 136 ng/ml, Fig. 3e). The increase in neutralizing activity between the first and second vaccine
171 dose was associated with a decrease in the percentage of non-neutralizing antibodies (defined as
172 IC50 >1000 ng/ml) and increased representation of neutralizing antibodies (p= 0.003, Fig. 3a). In
173 conclusion, memory B cells recruited after the second dose account for most of the improvement
174 in neutralizing activity in this compartment between the 2 vaccine doses. Thus, in addition to the
175 quantitative improvement in serum neutralizing activity there is also an improvement in the
176 neutralizing activity of the antibodies expressed in the memory compartment after boosting.

177

178 In contrast, there was no significant improvement in neutralizing activity of the monoclonal
179 antibodies obtained between 1.3 and 5 months after vaccination ($p>0.99$, Fig. 3a). Although there
180 was some improvement among B cell clones, which was accounted for by the small minority of
181 persisting clones, neither was significant ($p=0.58$ and 0.46, Fig. 3b-e, Supplementary table 6). In
182 contrast, memory antibodies obtained from convalescent individuals showed improved
183 neutralizing activity between 1.3[3] and 6.2 months[7] with IC_{50} of 171 ng/ml to 116 ng/ml (Fig. 3a),
184 which improved further after 1 year[1]. This improvement was due to increased neutralizing
185 activity among persisting clones ($p=0.003$, Fig. 3c).

186

187 **Affinity, Epitopes and Neutralization Breadth**

188 To examine affinity maturation after vaccination, we performed biolayer interferometry (BLI)
189 experiments using the Wuhan Hu-1 RBD[3]. 147 antibodies were assayed, 30 obtained after the
190 prime, 74 1.3-months after boosting, and 43 5-months after the boost. Geometric mean IC_{50}s
191 were comparable for the antibodies obtained from the 1.3- and 5-month time points (Extended
192 data Fig. 7a). Overall, there was a 3- and 7.5 fold increase in affinity between the antibodies
193 obtained between the first 2, and second 2 time points respectively (Fig. 4a). After 5 months the
194 affinity of the antibodies obtained from vaccinated individuals was similar to antibodies obtained
195 from naturally infected voluteers (Fig 4a). However, there was no correlation between affinity
196 and neutralizing activity of the antibodies tested at any of the 3 time points (Extended Data Fig.
197 7b).

198

199 We also compared the affinities of pairs of antibodies obtained from persisting clones between
200 1.3 and 5 months after vaccination. Persisting clones obtained at 1.3 and 5 months from
201 vaccinated individuals showed a median 4.5-fold increase in affinity ($p<0.0001$, Fig. 4b). In
202 contrast, a comparable group of persisting clonal antibodies obtained from convalescent
203 individuals 1.3 and 6.2 months after infection showed a median 11.2-fold increase in affinity
204 ($p=0.002$, Fig. 4b).
205
206 To determine whether the epitopes targeted by the monoclonal antibodies were changing over
207 time, we performed BLI experiments in which a preformed antibody-RBD complex was exposed
208 to a second monoclonal targeting one of 4 classes of structurally defined epitopes[1,3] (see
209 schematic in Extended data Fig. 8a). There was no significant change in the distribution of
210 targeted epitopes among 52 randomly selected antibodies with comparable neutralizing activity
211 obtained from the 1.3- and 5-month time points (Extended Data Fig. 8b and c, and Extended
212 Data Fig. 9).
213
214 In addition to the increase in potency, the neutralizing breath of memory antibodies obtained
215 from persisting clones from convalescent individuals increases with time after infection[1,7,25]. To
216 determine whether there is a similar increase in breadth with time after vaccination, we selected
217 20 random antibodies from the prime or 1.3 months after boost, with representative levels of
218 activity against the original Wuhan Hu-1 strain, and measured their neutralization potency
219 against a panel of pseudotypes encoding RBD mutations which were selected for resistance to
220 different RBD antibody classes and/or are associated with circulating variants of concern
221 (Extended data. Fig. 10). There was little change in breadth between prime and 1.3 months after

222 boost, with only a small increase in resistance to K417N and A475V substitutions (Extended
223 data Fig. 10, Supplementary Table 7).
224
225 In addition, we assayed 19 pairs of neutralizing antibodies expressed by persisting clones
226 obtained 1.3 and 5 months after vaccination against the same mutant pseudotype viruses (Fig. 4c
227 and Supplementary Table 8). They were compared to 7 previously reported[25], plus 9 additional
228 pairs of antibodies obtained from convalescent individuals at 1.3- and 6.2-month time points
229 (Fig. 4d and Supplementary Table 8). Whereas only 36 of 190 (19%) of the vaccinee antibody-
230 mutant combinations showed improved potency, 95 of the 160 (59%) convalescent pairs did so
231 ($p<0.0001$, Fig. 4c, d and e). Moreover, only 4 of the 19 (21%) vaccine antibody pairs showed
232 improved potency against pseudotypes carrying B.1.617.2 (delta variant)-specific RBD amino
233 acid substitutions (L452R/T478K), while 11 out of 16 (69%) of the convalescent antibody pairs
234 showed improved activity against this virus ($p=0.007$, Fig. 4c, d and e). We conclude that there is
235 less increase in breadth in the months after mRNA vaccination than in a similar interval in
236 naturally infected individuals.
237
238 Circulating antibodies are produced by an initial burst of short-lived plasmablasts[26-28], and
239 maintained by plasma cells with variable longevity[29-32]. SARS-CoV-2 infection or mRNA
240 vaccination produces an early peak antibody response that decreases by 5-10-fold after 5
241 months[7,33-37]. Notably, neutralization titres elicited by vaccination exceed those of COVID-19
242 recovered individuals at all comparable time points assayed. Nevertheless, neutralizing potency
243 against variants is significantly lower than against Wuhan Hu-1, with up to 5-10-fold reduced
244 activity against the B.1.351 variant[5,6,13,14,38]. Taken together with the overall decay in

245 neutralizing activity there can be 1-2 orders of magnitude decrease in serum neutralizing activity
246 after 5 or 6 months against variants when compared to the peak of neutralizing activity against
247 Wuhan Hu-1. Thus, antibody mediated protection against variants is expected to wane
248 significantly over a period of months, consistent with reports of reinfection in convalescent
249 individuals and breakthrough infection by variants in fully vaccinated individuals[39-42].
250
251 In contrast to circulating antibodies, memory B cells are responsible for rapid recall responses[43-
252 46], and the number of cells in this compartment is relatively stable over the first 5-6 months after
253 mRNA vaccination or natural infection[7,47]. In both cases memory B cells continue to evolve as
254 evidenced by increasing levels of somatic mutation and emergence of unique clones.
255
256 The memory response would be expected to protect individuals that suffer breakthrough
257 infection from developing serious disease. Both natural infection and mRNA vaccination
258 produce memory antibodies that evolve increased affinity. However, vaccine-elicited memory
259 monoclonal antibodies show more modest neutralizing potency and breadth than those that
260 developed after natural infection[1,7]. Notably, the difference between the memory compartment
261 that develops in response to natural infection vs mRNA vaccination reported above is consistent
262 with the higher level of protection from variants conferred by natural infection[42].
263
264 There are innumerable differences between natural infection and mRNA vaccination that could
265 account for the differences in antibody evolution over time. These include but are not limited to:
266 1. Route of antigen delivery, respiratory tract vs. intra-muscular injection[48,49]; 2. The physical
267 nature of the antigen, intact virus vs. conformationally stabilized prefusion S protein[50]; 3.

268 Antigen persistence, weeks in the case of natural infection[7] vs. hours to days for mRNA[51]. Each
269 of these could impact on B cell evolution and selection directly, and indirectly through
270 differential T cell recruitment.
271
272 The increase in potency and breadth in the memory compartment that develops after natural
273 infection accounts for the exceptional responses to Wuhan Hu-1 and its variants that
274 convalescent individuals develop when boosted with mRNA vaccines[1,5]. The expanded memory
275 B cell compartment in mRNA vaccinees should also produce high titers of neutralizing
276 antibodies when vaccinees are boosted or when they are re-exposed to the virus[52]. Boosting
277 vaccinated individuals with currently available mRNA vaccines should produce strong responses
278 that mirror or exceed their initial vaccine responses to Wuhan-Hu but with similarly decreased
279 coverage against variants. Whether an additional boost with Wuhan-Hu-based or variant
280 vaccines or re-infection will also elicit development of memory B cells expressing antibodies
281 showing increased breadth remains to be determined. Finally, timing an additional boost for
282 optimal responses depends on whether the objective is to prevent infection or disease[53]. Given
283 the current rapid emergence of SARS-CoV-2 variants, boosting to prevent infection would likely
284 be needed on a time scale of months. The optimal timing for boosting to prevent serious disease
285 will depend on the stability and further evolution of the memory B cell compartment.
286

287 **FIGURES**

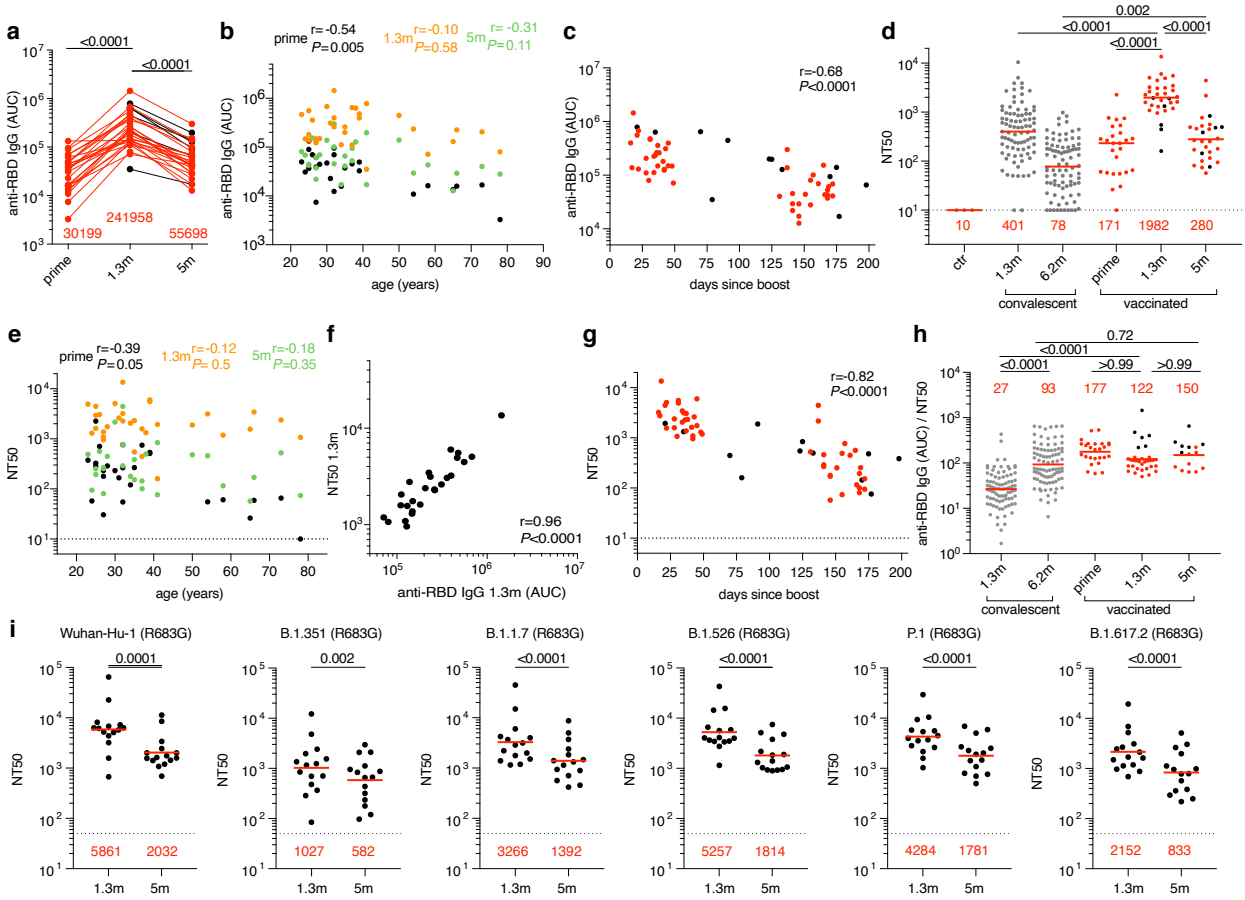

288

289 **Fig. 1: Plasma ELISAs and neutralizing activity.**

290 **a,** Graph shows area under the curve (AUC, Y-axis) for plasma IgG antibody binding to SARS-
291 CoV-2 RBD after prime, and 1.3 months (m) and 5 months (m) post-second vaccination for n=32
292 paired samples. Samples without a prime value are shown in black (n=6). **b**, Graph shows plasma
293 IgG antibody binding (AUC, Y-axis) plotted against age (X-axis) after prime (black), and 1.3
294 months (orange) and 5 months (green) post-second vaccination. **c**, Graph shows AUC values from
295 **a** (Y-axis) plotted against time after vaccination (X-axis). Samples without a prime value are
296 shown in black. **d,** NT50 values in pre-pandemic plasma (ctr) as well as plasma from convalescent
297 individuals 1.3m[3] and 6.2m[7] after infection (grey) and in n=32 vaccinated individuals after prime,
298 and 1.3- and 5-months after receiving 2 doses of an mRNA vaccine. Samples without a prime

299 value are shown in black. **e**, NT50 values (Y-axis) vs. age (years, X-axis) in individuals after prime
300 (black), or 1.3 months (1.3m, orange) or 5 months (5m, green) after boosting with an mRNA
301 vaccine. **f**, NT50 values (Y-axis) vs. IgG antibody binding (AUC, X-axis) 1.3 months after 2 doses
302 of an mRNA vaccine (n=26). **g,** Graph shows NT50 values (Y-axis) vs. days after boost (X-axis)
303 in individuals receiving two doses of an mRNA vaccine. Samples without a prime value are shown
304 in black. **h,** Ratio of anti-RBD IgG antibody (AUC) to NT50 values (Y-axis) plotted for
305 convalescent infected individuals (grey) 1.3m[3] or 6.2m[7] after infection, and vaccinated individuals
306 after the prime, and 1.3m and 5m after receiving 2 doses of an mRNA vaccine. Samples without a
307 prime value are shown in black. **i**, Plasma neutralizing activity against indicated SARS-CoV-2
308 variants of interest/concern (n=15 paired samples at 1.3- and 5-months after full vaccination).
309 Refer to Methods for a list of all substitutions/deletions/insertions in the spike variants. All
310 experiments were performed at least in duplicate. Red bars and values in **a, d, h** and **i** represent
311 geometric mean values. Statistical significance in **a, d, h** and **i** was determined by Kruskal-Wallis
312 test with subsequent Dunn's multiple comparisons, and in **b, c, e, f,** and **g** by Spearman correlation
313 test.
314
315

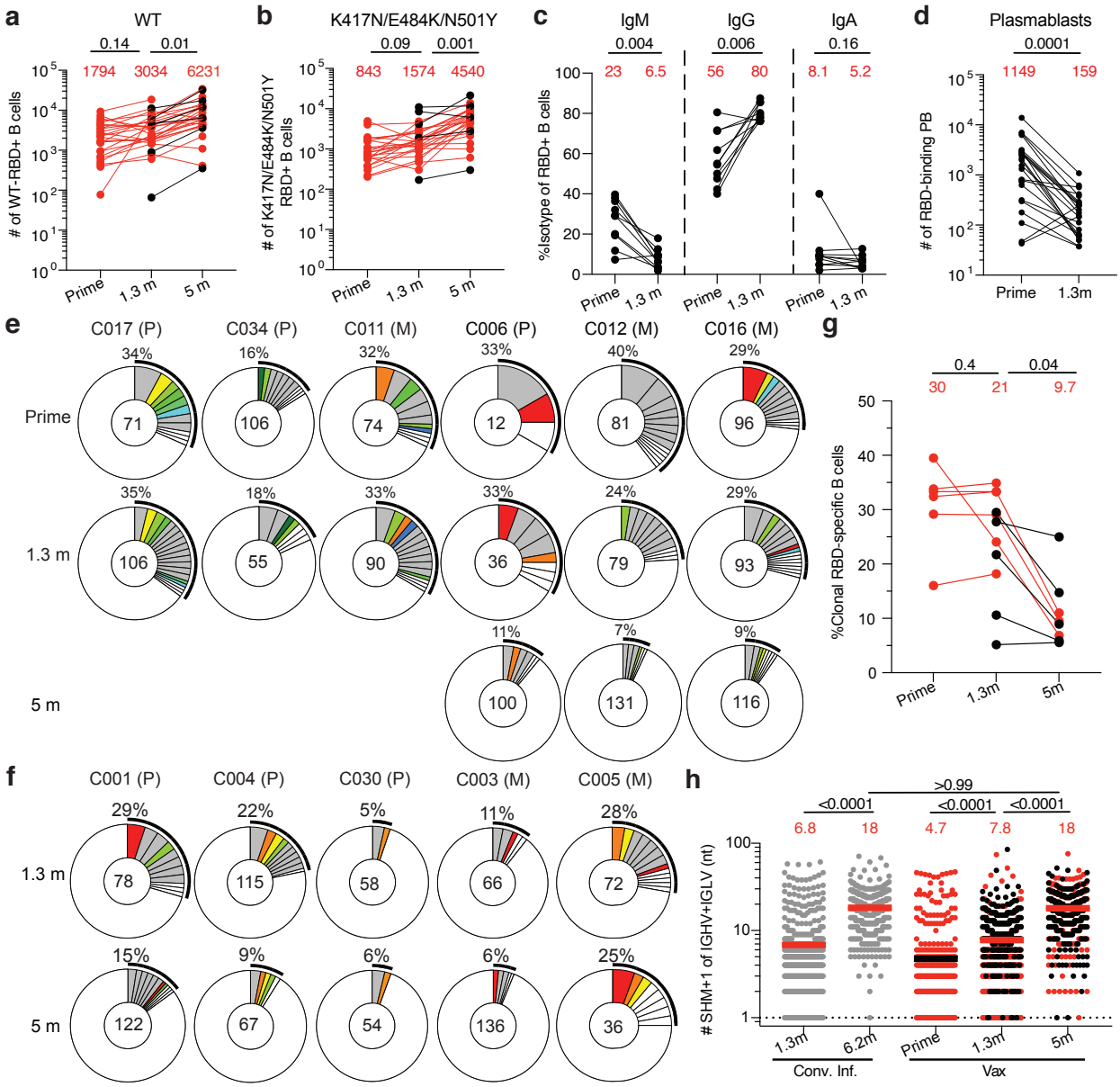

Fig. 2: Anti-SARS-CoV-2 RBD B cells after vaccination. a-d, Graphs summarizing **a,** the number of Wuhan-Hu RBD (WT)-specific memory B cells per 10 million B cells for vaccinees and **b,** the number of antigen-specific memory B cells cross-reactive with both WT and K417N/E484K/N501Y RBD mutant per 10 million B cells for n=32 vaccinated individuals after prime, 1.3- and 5-months after 2 doses of vaccination. Samples without a prime value are shown in black. **c,** the frequency of IgM, IgG, or IgA isotype expression by Wuhan-Hu RBD-specific memory B cells after prime or 1.3 months post-boost (n=10), and **d,** number of Wuhan-Hu RBD-

binding plasmablasts per 10 million B cells (n=26) after prime or 1.3 months post-boost. Red numbers indicate geometric means. Gating strategy is in Extended Data Fig. 2. **e, and f,** Pie charts show the distribution of IgG antibody sequences obtained from memory B cells from 11 individuals after **e,** prime and 1.3-months or 5-months post-boost and **f,** 1.3- and 5-months post-boost. The number inside the circle indicates the number of sequences analyzed for the individual denoted above the circle, with Pfizer vaccinees indicated by (P) and Moderna by (M). Pie slice size is proportional to the number of clonally related sequences. The black outline and associated numbers indicate the percentage of clonally expanded sequences detected at each time point. Colored slices indicate persisting clones (same *IGHV* and *IGLV* genes, with highly similar CDR3s) found at more than one timepoint within the same individual. Grey slices indicate clones unique to the timepoint. White slices indicate repeating sequences isolated only once per time point. **g,** Graph shows the relative percentage of clonal sequences at each time point in **e** and **f**. The red numbers indicate the geometric means. Samples without a prime value are shown in black. **h,** Number of nucleotide somatic hypermutations (SHM) in the *IGHV* and *IGLV* combined (also Supplementary Table 4) in the antibodies illustrated in **e** and **f**, compared to the number of mutations obtained after 1.3[3] or 6.2[7] months after infection (grey)**.** Horizontal bars and red numbers indicate mean number of nucleotide mutations at each time point. Samples without a prime value are shown in black. Statistical significance in **a, b, g,** and **h** was determined by Kruskal Wallis test with subsequent Dunn's multiple comparisons, and in **c** and **d** was determined using Wilcoxon matched-pairs signed rank test.

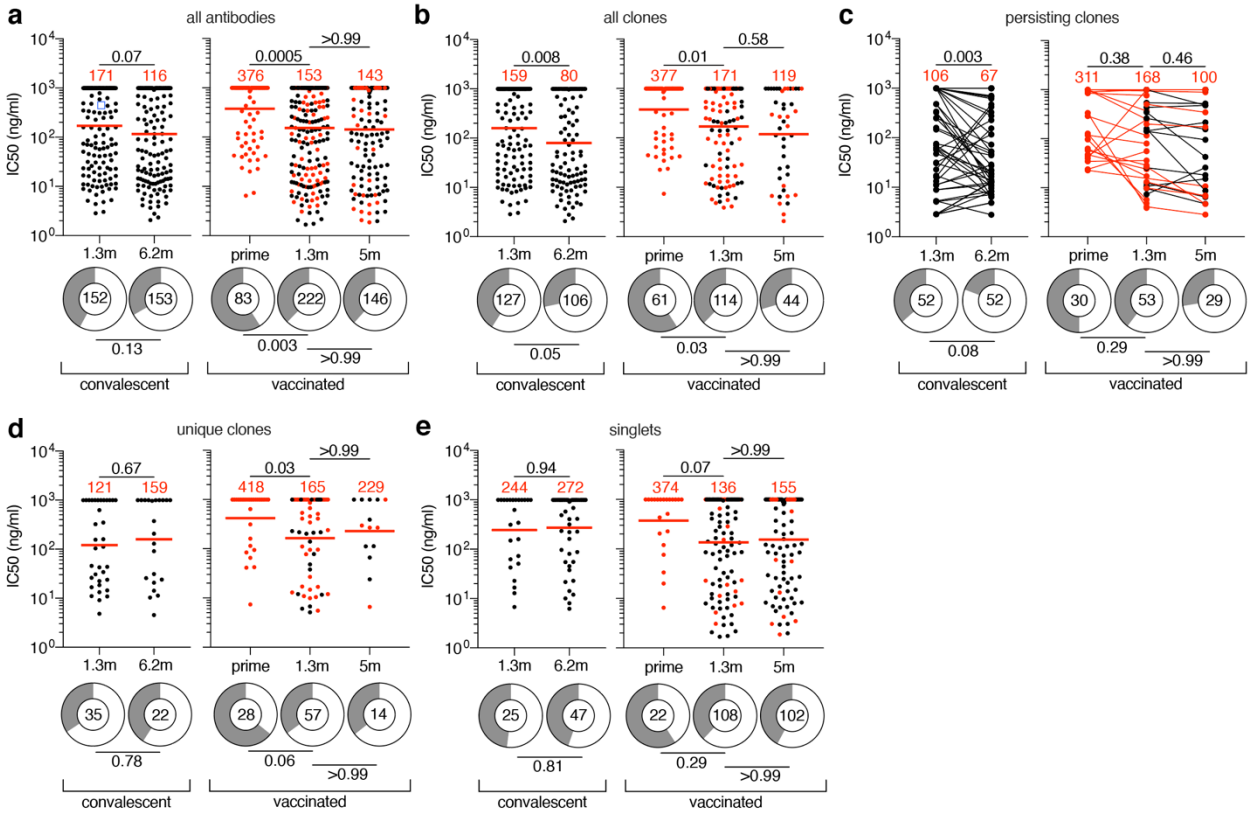

346

347 **Fig. 3: Anti-SARS-CoV-2 RBD monoclonal antibodies. a-e,** Graphs show anti-SARS-CoV-2
348 neutralizing activity of monoclonal antibodies measured by a SARS-CoV-2 pseudotype virus
349 neutralization assay using wild-type (Wuhan Hu-1[54]) SARS-CoV-2 pseudovirus[3,8]. Half-maximal
350 inhibitory concentration (IC_{50}) values for all antibodies (**a**), all clones (**b**), persisting clones (**c**),
351 unique clones (**d**) and singlets (**e**) isolated from COVID-19 convalescent individuals 1.3[3] and 6.2[7]
352 months after infection or from vaccinated individuals after prime, and 1.3- or 5-months after 2
353 doses of vaccine. Each dot represents one antibody, where 451 total antibodies were tested
354 including the 430 reported herein (Supplementary Table 5), and 21 previously reported antibodies
355 derived from vaccinees within 8 weeks post-vaccination[13]. Antibodies isolated from samples
356 without a prime value are shown in black. Pie charts illustrate the fraction of non-neutralizing
357 (IC50 > 1000 ng/ml) antibodies (grey slices), inner circle shows the number of antibodies tested

per group. Horizontal bars and red numbers indicate geometric mean values. Statistical significance was determined by Kruskal Wallis test with subsequent Dunn's multiple comparisons. Statistical significance for ring plots was determined using Fisher's exact test with subsequent Bonferroni-correction. All experiments were performed at least twice.

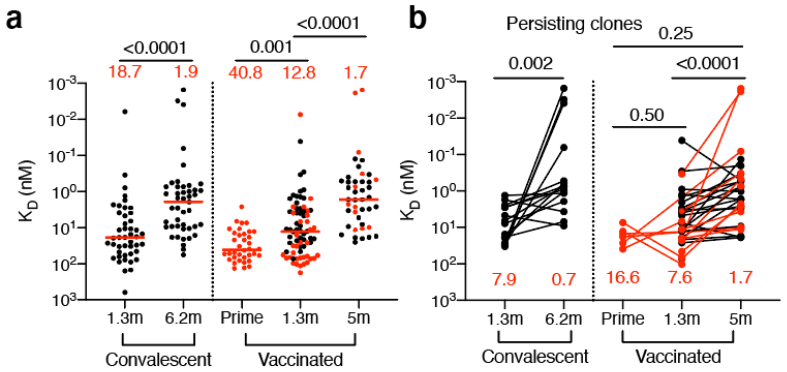

c Vaccination persisting clones 1.3m/5m

	wt	R683G	R346S	K417N	N440K	A475V	E484K R683G	Q493R	N501Y	KEN R683G	L452R E484Q R683G	L452R T478K R683G
C1332	5	4	8	7	6	5	5	6	5	4	4	5
C2464	12	2	20	42	12	12	2	1	7	1	93	1
C2431	14	12	30	100	25	1	8	4	15	100	13	21
C1207	103	68	121	86	125	19	61	58	26	3	61	61
C1189	113	103	129	6	112	78	5	80	77	73	8	76
C2460	153	110	163	4	158	244	321	321	205	15	239	154
C2394	261	58	5	393	256	296	100	220	278	100	100	1
C1213	101	101	14	178	164	148	52	132	133	48	100	100
C1344	77	13	77	96	66	100	93	50	82	78	78	83
C2409	95	71	100	35	47	82	47	72	70	54	78	81
C2471	32	41	84	65	75	54	46	49	55	61	64	103
C1335	48	79	73	54	68	48	86	64	50	61	141	105
C1333	86	99	97	87	89	84	95	109	93	88	92	114
C1330	84	42	100	45	100	80	98	100	100	100	83	100
C2479	95	96	106	89	100	59	88	106	113	97	106	100
C1334	65	107	173	88	109	82	99	95	66	79	112	111
C1211	115	113	165	109	188	142	122	105	126	125	130	128
C1302	85	21	70	588	64	109	77	97	102	529	78	107
C1187	431	196	134	310	480	126	149	1257	574	186	126	151

%IC50 of shared clone isolated 1.3m after vaccination

d Convalescent infection persisting clones 1.3m/6.2m

	wt	R683G	R346S	K417N	N440K	A475V	E484K R683G	Q493R	N501Y	KEN R683G	L452R E484Q R683G	L452R T478K R683G
C542	2	4	2	1	2	2	1	2	1	13	1	2
C099	3	1	4	2	3	2	1	5	8	0.4	2	1
C513	16	5	19	9	10	4	15	15	15	5	4	2
C573	1	5	100	1	1	1	2	1	2	1	2	4
C043	18	2.9	17	51	13	4	1	0.3	14	2	1	3
C512	10	2	100	2	25	7	0.3	9	53	0.2	1	2
C055	2	1	2	3	2	1	42	1	1	30	1	100
C080	70	69	3	11	4	35	10	68	71	20	1	1
C549	29	6	62	38	46	44	4	1	15	34	0.1	1
C511	83	45	101	34	71	3	24	10	1	0.2	25	23
C057	47	43	38	35	30	30	89	4	22	100	0.1	31
C095	88	19	121	15	44	57	100	0.3	81	100	100	0.2
C502	154	61	169	136	97	124	100	1	126	100	100	1
C572	148	28	96	60	127	138	100	100	401	144	248	184
C051	295	49	525	293	412	241	52	1	419	100	7	34
C052	48	112	37	50	36	35	192	457	27	100	100	41

%IC50 of shared clone isolated 1.3m after infection

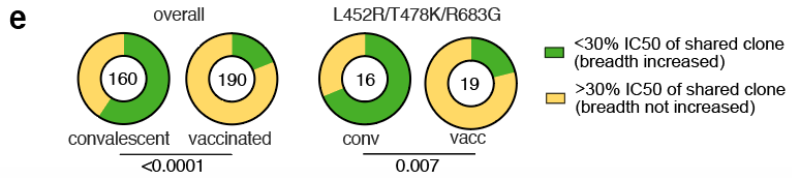

365 **Fig. 4: Affinity and Breadth. a-b,** Graphs show antibody K_Ds for Wuhan-Hu RBD measured by
366 BLI. **a,** antibodies isolated from convalescent individuals 1.3[3]- (n=42) and 6.2-months[7] (n=45)
367 after infection or from vaccinees after prime (n=36), and 1.3- (n=74) and 5-months (n=43) post-
368 second vaccination. **b**, Clonally-paired antibodies isolated from convalescent individuals 1.3[3]- and
369 6.2[7]-months after infection (n=15) or vaccinated individuals between prime and 1.3 month (n=3),
370 prime and 5 months (n=3), or 1.3- and 5-months after full vaccination (n=26). Antibodies isolated
371 from samples without a prime value are shown in black. Red horizontal bars and numbers indicate
372 median values. Statistical significance was determined using Kruskal Wallis test with subsequent
373 Dunn's multiple comparisons. **c-d,** Heat-maps show inhibitory concentrations of antibodies
374 isolated 5m after vaccination (**c**) or 6.2m[7] after infection (**d**) normalized to their shared clone
375 isolated 1.3m after vaccination (**c**) or 1.3m[3] after infection (**d**), expressed as %IC50, against
376 indicated mutant SARS-CoV-2 pseudoviruses (Supplementary Table 8). Antibodies with
377 improved (<30%) IC50 compared to their clonal relative isolated at an earlier timepoint are colored
378 in shades of green with most improved antibodies in darkest green. Antibodies with worse
379 (>300%) IC50 than their clonal relative isolated at an earlier timepoint are colored in red with the
380 most worsened antibodies in dark red. Antibodies that did not change their IC50 by more than ~3-
381 fold are shown in yellow. **e,** Pie charts illustrate the fraction of antibodies showing improved
382 (<30%, green) vs. not improved (yellow) IC_{50} compared to their clonal relative isolated at an earlier
383 timepoint, inner circle shows the number of antibody-mutant combinations analyzed per group.
384 Statistical significance for ring plots was determined using Fisher's exact test.

385

386

387 **METHODS**

388

389 **Study participants**.

390 Participants were healthy volunteers receiving either the Moderna (mRNA-1273) or Pfizer-
391 BioNTech (BNT162b2) mRNA vaccines against severe acute respiratory syndrome coronavirus 2
392 (SARS-CoV-2) who were recruited for serial blood donations at Rockefeller University Hospital
393 in New York between January 21 and July 20, 2021. The majority of participants (n=28) were *de*
394 *novo* recruited for this study, while a subgroup of individuals (n=4) were from a long-term study
395 cohort[13]. Eligible participants were healthy adults with no history of infection with SARS-CoV-2,
396 as determined by clinical history and confirmed through serology testing, receiving one of the two
397 Moderna (mRNA-1273) or Pfizer-BioNTech (BNT162b2), according to current dosing and
398 interval guidelines. Exclusion criteria included incomplete vaccination status, presence of clinical
399 signs and symptoms suggestive of acute infection with or a positive reverse transcription
400 polymerase chain reaction (RT-PCR) results for SARS-CoV-2 in saliva, or a positive (coronavirus
401 disease 2019) COVID-19 serology. Seronegativity for COVID-19 was established through the
402 absence of serological activity toward the nucleocapsid protein (N) of SARS-CoV-2. Participants
403 presented to the Rockefeller University Hospital for blood sample collection and were asked to
404 provide details of their vaccination regimen, possible side effects, comorbidities and possible
405 COVID-19 history. All participants provided written informed consent before participation in the
406 study and the study was conducted in accordance with Good Clinical Practice. The study was
407 performed in compliance with all relevant ethical regulations and the protocol (DRO-1006) for
408 studies with human participants was approved by the Institutional Review Board of the Rockefeller
409 University. For detailed participant characteristics see Supplementary Tables 1 and 2.

410

411 **Blood samples processing and storage.**

412 Peripheral Blood Mononuclear Cells (PBMCs) obtained from samples collected at Rockefeller
413 University were purified as previously reported by gradient centrifugation and stored in liquid
414 nitrogen in the presence of Fetal Calf Serum (FCS) and Dimethylsulfoxide (DMSO)[3,7].
415 Heparinized plasma and serum samples were aliquoted and stored at -20°C or less. Prior to
416 experiments, aliquots of plasma samples were heat-inactivated (56°C for 1 hour) and then stored
417 at 4°C.

418

419 **ELISAs**

420 Enzyme-Linked Immunosorbent Assays (ELISAs)[55,56] to evaluate antibodies binding to SARS-
421 CoV-2 RBD were performed by coating of high-binding 96-half-well plates (Corning 3690) with
422 50 µl per well of a 1µg/ml protein solution in Phosphate-buffered Saline (PBS) overnight at 4°C.
423 Plates were washed 6 times with washing buffer (1× PBS with 0.05% Tween-20 (Sigma-
424 Aldrich)) and incubated with 170 µl per well blocking buffer (1× PBS with 2% BSA and 0.05%
425 Tween-20 (Sigma)) for 1 hour at room temperature. Immediately after blocking, monoclonal
426 antibodies or plasma samples were added in PBS and incubated for 1 hour at room temperature.
427 Plasma samples were assayed at a 1:66 starting dilution and 10 additional threefold serial
428 dilutions. Monoclonal antibodies were tested at 10 µg/ml starting concentration and 10 additional
429 fourfold serial dilutions. Plates were washed 6 times with washing buffer and then incubated
430 with anti-human IgG, IgM or IgA secondary antibody conjugated to horseradish peroxidase
431 (HRP) (Jackson Immuno Research 109-036-088 109-035-129 and Sigma A0295) in blocking
432 buffer at a 1:5,000 dilution (IgM and IgG) or 1:3,000 dilution (IgA). Plates were developed by

433 addition of the HRP substrate, 3,3',5,5'-Tetramethylbenzidine (TMB) (ThermoFisher) for 10
434 minutes (plasma samples) or 4 minutes (monoclonal antibodies). The developing reaction was
435 stopped by adding 50 µl of 1 M H_2SO_4 and absorbance was measured at 450 nm with an ELISA
436 microplate reader (FluoStar Omega, BMG Labtech) with Omega and Omega MARS software for
437 analysis. For plasma samples, a positive control (plasma from participant COV72, diluted 66.6-
438 fold and ten additional threefold serial dilutions in PBS) was added to every assay plate for
439 normalization. The average of its signal was used for normalization of all the other values on the
440 same plate with Excel software before calculating the area under the curve using Prism
441 V9.1(GraphPad). Negative controls of pre-pandemic plasma samples from healthy donors were
442 used for validation (for more details please see[3]). For monoclonal antibodies, the ELISA half-
443 maximal concentration (EC50) was determined using four-parameter nonlinear regression
444 (GraphPad Prism V9.1). EC50s above 2000 ng/mL were considered non-binders.
445
446 **Proteins**
447 The mammalian expression vector encoding the Receptor Binding-Domain (RBD) of SARS-
448 CoV-2 (GenBank MN985325.1; Spike (S) protein residues 319-539) was previously described[57].
449
450 **SARS-CoV-2 pseudotyped reporter virus**
451 A panel of plasmids expressing RBD-mutant SARS-CoV-2 spike proteins in the context of
452 pSARS-CoV-2-S $_{\Delta 19}$ has been described[13,25,58]. Variant pseudoviruses resembling variants of
453 interest/concern B.1.1.7 (first isolated in the UK), B.1.351 (first isolated in South-Africa),
454 B.1.526 (first isolated in New York City), P.1 (first isolated in Brazil) and B.1.617.2 (first
455 isolated in India) were generated by introduction of substitutions using synthetic gene fragments

456 (IDT) or overlap extension PCR mediated mutagenesis and Gibson assembly. Specifically, the
457 variant-specific deletions and substitutions introduced were:
458 B.1.1.7: ΔH69/V70, ΔY144, N501Y, A470D, D614G, P681H, T761I, S982A, D118H
459 B.1.351: D80A, D215G, L242H, R246I, K417N, E484K, N501Y, D614G, A701V
460 B.1.526: L5F, T95I, D253G, E484K, D614G, A701V.
461 P.1: L18F, T20N, P26S, D138Y, R190S, K417T, E484K, N501Y, D614G, H655Y, T1027I,
462 V1167F
463 B.1.617.2: T19R, Δ156-158, L452R, T478K, D614G, P681R, D950N
464 The E484K, K417N/E484K/N501Y, L452R/E484Q and L452R/T478K substitution, as well as
465 the deletions/substitutions corresponding to variants of concern listed above were incorporated
466 into a spike protein that also includes the R683G substitution, which disrupts the furin cleaveage
467 site and increases particle infectivity. Neutralizing activity against mutant pseudoviruses were
468 compared to a wildtype (WT) SARS-CoV-2 spike sequence (NC_045512), carrying R683G
469 where appropriate.
470
471 SARS-CoV-2 pseudotyped particles were generated as previously described[3,8]. Briefly, 293T
472 cells were transfected with pNL4-3ΔEnv-nanoluc and pSARS-CoV-2-$S_{\Delta 19}$, particles were
473 harvested 48 hours post-transfection, filtered and stored at -80°C.
474
475 **Pseudotyped virus neutralization assay**
476 Fourfold serially diluted pre-pandemic negative control plasma from healthy donors, plasma
477 from COVID-19-convalescent individuals or monoclonal antibodies were incubated with SARS-
478 CoV-2 pseudotyped virus for 1 hour at 37 °C. The mixture was subsequently incubated with

479 $293T_{Ace2}$ cells[3] (for all WT neutralization assays) or HT1080Ace2 cl14 (for all mutant panels and
480 variant neutralization assays) cells[13] for 48 hours after which cells were washed with PBS and
481 lysed with Luciferase Cell Culture Lysis 5× reagent (Promega). Nanoluc Luciferase activity in
482 lysates was measured using the Nano-Glo Luciferase Assay System (Promega) with the Glomax
483 Navigator (Promega). The relative luminescence units were normalized to those derived from
484 cells infected with SARS-CoV-2 pseudotyped virus in the absence of plasma or monoclonal
485 antibodies. The half-maximal neutralization titers for plasma (NT_{50}) or half-maximal and 90%
486 inhibitory concentrations for monoclonal antibodies (IC_{50} and IC_{90}) were determined using four-
487 parameter nonlinear regression (least squares regression method without weighting; constraints:
488 top=1, bottom=0) (GraphPad Prism).
489
490 **Biotinylation of viral protein for use in flow cytometry**
491 Purified and Avi-tagged SARS-CoV-2 RBD or SARS-CoV-2 RBD K417N/E484K/N501Y
492 mutant was biotinylated using the Biotin-Protein Ligase-BIRA kit according to manufacturer's
493 instructions (Avidity) as described before[3]. Ovalbumin (Sigma, A5503-1G) was biotinylated
494 using the EZ-Link Sulfo-NHS-LC-Biotinylation kit according to the manufacturer's instructions
495 (Thermo Scientific). Biotinylated ovalbumin was conjugated to streptavidin-BV711 (BD
496 biosciences, 563262) and RBD to streptavidin-PE (BD Biosciences, 554061) and streptavidin-
497 AF647 (Biolegend, 405237)[3].
498
499 **Flow cytometry and single cell sorting**
500 Single-cell sorting by flow cytometry was described previously[3]. Briefly, peripheral blood
501 mononuclear cells were enriched for B cells by negative selection using a pan-B-cell isolation kit

502 according to the manufacturer's instructions (Miltenyi Biotec, 130-101-638). The enriched B
503 cells were incubated in Flourescence-Activated Cell-sorting (FACS) buffer (1× PBS, 2% FCS, 1
504 mM ethylenediaminetetraacetic acid (EDTA)) with the following anti-human antibodies (all at
505 1:200 dilution): anti-CD20-PECy7 (BD Biosciences, 335793), anti-CD3-APC-eFluro 780
506 (Invitrogen, 47-0037-41), anti-CD8-APC-eFluor 780 (Invitrogen, 47-0086-42), anti-CD16-APC-
507 eFluor 780 (Invitrogen, 47-0168-41), anti-CD14-APC-eFluor 780 (Invitrogen, 47-0149-42), as
508 well as Zombie NIR (BioLegend, 423105) and fluorophore-labeled RBD and ovalbumin (Ova)
509 for 30 min on ice. Single CD3-CD8-CD14-CD16−CD20+Ova−RBD-PE+RBD-AF647+ B cells
510 were sorted into individual wells of 96-well plates containing 4 µl of lysis buffer (0.5× PBS, 10
511 mM Dithiothreitol (DTT), 3,000 units/ml RNasin Ribonuclease Inhibitors (Promega, N2615) per
512 well using a FACS Aria III and FACSDiva software (Becton Dickinson) for acquisition and
513 FlowJo for analysis. The sorted cells were frozen on dry ice, and then stored at −80 °C or
514 immediately used for subsequent RNA reverse transcription. For plasmablast single-cell sorting,
515 in addition to above antibodies, B cells were also stained with anti-CD19-BV605 (Biolegend,
516 302244), and single CD3-CD8-CD14-CD16-CD19+CD20-Ova-RBD-PE+RBD-AF647+
517 plasmablasts were sorted as described above. For B cell phenotype analysis, in addition to above
518 antibodies, B cells were also stained with following anti-human antibodies: anti-IgD-BV421
519 (Biolegend, 348226), anti-CD27-FITC (BD biosciences, 555440), anti-CD19-BV605
520 (Biolegend, 302244), anti-CD71- PerCP-Cy5.5 (Biolegend, 334114), anti- IgG-PECF594 (BD
521 biosciences, 562538), anti-IgM-AF700 (Biolegend, 314538), anti-IgA-Viogreen (Miltenyi
522 Biotec, 130-113-481).
523
524 **Antibody sequencing, cloning and expression**

525 Antibodies were identified and sequenced as described previously[3,59]. In brief, RNA from single
526 cells was reverse-transcribed (SuperScript III Reverse Transcriptase, Invitrogen, 18080-044) and
527 the cDNA was stored at −20 °C or used for subsequent amplification of the variable IGH, IGL
528 and IGK genes by nested PCR and Sanger sequencing. Sequence analysis was performed using
529 MacVector. Amplicons from the first PCR reaction were used as templates for sequence- and
530 ligation-independent cloning into antibody expression vectors. Recombinant monoclonal
531 antibodies were produced and purified as previously described[3].
532
533 **Biolayer interferometry**
534 Biolayer interferometry assays were performed as previously described[3]. Briefly, we used the
535 Octet Red instrument (ForteBio) at 30 °C with shaking at 1,000 r.p.m. Affinity measurement of
536 anti-SARS-CoV-2 IgGs binding were corrected by subtracting the signal obtained from traces
537 performed with IgGs in the absence of WT RBD. The kinetic analysis using protein A biosensor
538 (ForteBio 18-5010) was performed as follows: (1) baseline: 60sec immersion in buffer. (2)
539 loading: 200sec immersion in a solution with IgGs 10 μg/ml. (3) baseline: 200sec immersion in
540 buffer. (4) Association: 300sec immersion in solution with WT RBD at 20, 10 or 5 μg/ml (5)
541 dissociation: 600sec immersion in buffer. Curve fitting was performed using a fast 1:1 binding
542 model and the Data analysis software (ForteBio). Mean equilibrium dissociation constant (K_D)
543 values were determined by averaging all binding curves that matched the theoretical fit with an
544 R^2 value ≥ 0.8.
545
546 **Computational analyses of antibody sequences**

547 Antibody sequences were trimmed based on quality and annotated using Igblastn v.1.14. with
548 IMGT domain delineation system. Annotation was performed systematically using Change-O
549 toolkit v.0.4.540[60]. Heavy and light chains derived from the same cell were paired, and
550 clonotypes were assigned based on their V and J genes using in-house R and Perl scripts. All
551 scripts and the data used to process antibody sequences are publicly available on GitHub
552 (https://github.com/stratust/igpipeline/tree/igpipeline2_timepoint_v2).
553
554 The frequency distributions of human V genes in anti-SARS-CoV-2 antibodies from this study
555 was compared to 131,284,220 IgH and IgL sequences generated by[61] and downloaded from cAb-
556 Rep[62], a database of human shared BCR clonotypes available at https://cab-
557 rep.c2b2.columbia.edu/. Based on the 112 distinct V genes that make up the 7936 analyzed
558 sequences from Ig repertoire of the 11 participants present in this study, we selected the IgH and
559 IgL sequences from the database that are partially coded by the same V genes and counted them
560 according to the constant region. The frequencies shown in Extended Data Fig. 4 are relative to
561 the source and isotype analyzed. We used the two-sided binomial test to check whether the
562 number of sequences belonging to a specific *IGHV* or *IGLV* gene in the repertoire is different
563 according to the frequency of the same IgV gene in the database. Adjusted p-values were
564 calculated using the false discovery rate (FDR) correction. Significant differences are denoted
565 with stars.
566
567 Nucleotide somatic hypermutation and Complementarity-Determining Region (CDR3) length
568 were determined using in-house R and Perl scripts. For somatic hypermutations, *IGHV* and *IGLV*
569 nucleotide sequences were aligned against their closest germlines using Igblastn and the number

570 of differences were considered nucleotide mutations. The average number of mutations for V
571 genes was calculated by dividing the sum of all nucleotide mutations across all participants by
572 the number of sequences used for the analysis.
573
574 **Data availability statement:** Data are provided in Supplementary Tables 1-8. The raw
575 sequencing data and computer scripts associated with Figure 2 and Extended Data Fig. 3 have
576 been deposited at Github (https://github.com/stratust/igpipeline/tree/igpipeline2_timepoint_v2).
577 This study also uses data from "A Public Database of Memory and Naive B-Cell Receptor
578 Sequences" (https://doi.org/10.5061/dryad.35ks2), PDB (6VYB and 6NB6) and from "High
579 frequency of shared clonotypes in human B cell receptor repertoires"
580 (https://doi.org/10.1038/s41586-019-0934-8).
581
582 **Code availability statement:** Computer code to process the antibody sequences is available at
583 GitHub (https://github.com/stratust/igpipeline/tree/igpipeline2_timepoint_v2).
584
585
586 **Data presentation**
587 Figures arranged in Adobe Illustrator 2020.
588
589 **Competing interests:** The Rockefeller University has filed a provisional patent application in
590 connection with this work on which M.C.N.is an inventor (US patent 63/021,387). The patent
591 has been licensed by Rockefeller University to Bristol Meyers Squib.
592

593 **Acknowledgments:** We thank all study participants who devoted time to our research; The
594 Rockefeller University Hospital nursing staff and Clinical Research Support Office and nursing
595 staff. Mayu Okawa Frank, Marissa Bergh, and Robert B. Darnell for SARS-CoV-2 saliva PCR
596 testing. Charles M. Rice, and all members of the M.C.N. laboratory for helpful discussions, Maša
597 Jankovic for laboratory support, and Kristie Gordon for technical assistance with cell-sorting
598 experiments. This work was supported by NIH grant P01-AI138398-S1 (M.C.N.) and
599 2U19AI111825 (M.C.N.). R37-AI64003 to P.D.B.; R01AI78788 to T.H. F.M. is supported by
600 the Bulgari Women & Science Fellowship in COVID-19 Research. C.G. was supported by the
601 Robert S. Wennett Post-Doctoral Fellowship. D.S.B and C.G. were supported in part by the
602 National Center for Advancing Translational Sciences (National Institutes of Health Clinical and
603 Translational Science Award program, grant UL1 TR001866), and C.G. by the Shapiro-
604 Silverberg Fund for the Advancement of Translational Research. P.D.B. and M.C.N. are
605 Howard Hughes Medical Institute Investigators.

606

607 **Author Contributions:** P.D.B., T.H., and M.C.N. conceived, designed and analyzed
608 the experiments. M. Caskey and C.G. designed clinical protocols. A.C, F.M., D.S.B., Z.W., S.F.,
609 P.M., M.A., E.B., J.D.S., I.S., J.D. F.S., F.Z., and T.B.T. carried out experiments. A.G. and M.
610 Cipolla produced antibodies. D.S.B., M.D., M.T., K.G.M., C.G. and M. Caskey recruited
611 participants, executed clinical protocols. T.Y.O. and V.R. performed bioinformatic
612 analysis. A.C., F.M, D.S.B., Z.W., S.F., and M.C.N. wrote the manuscript with input from all
613 co-authors.

614

615 **EXTENDED FIGURES**

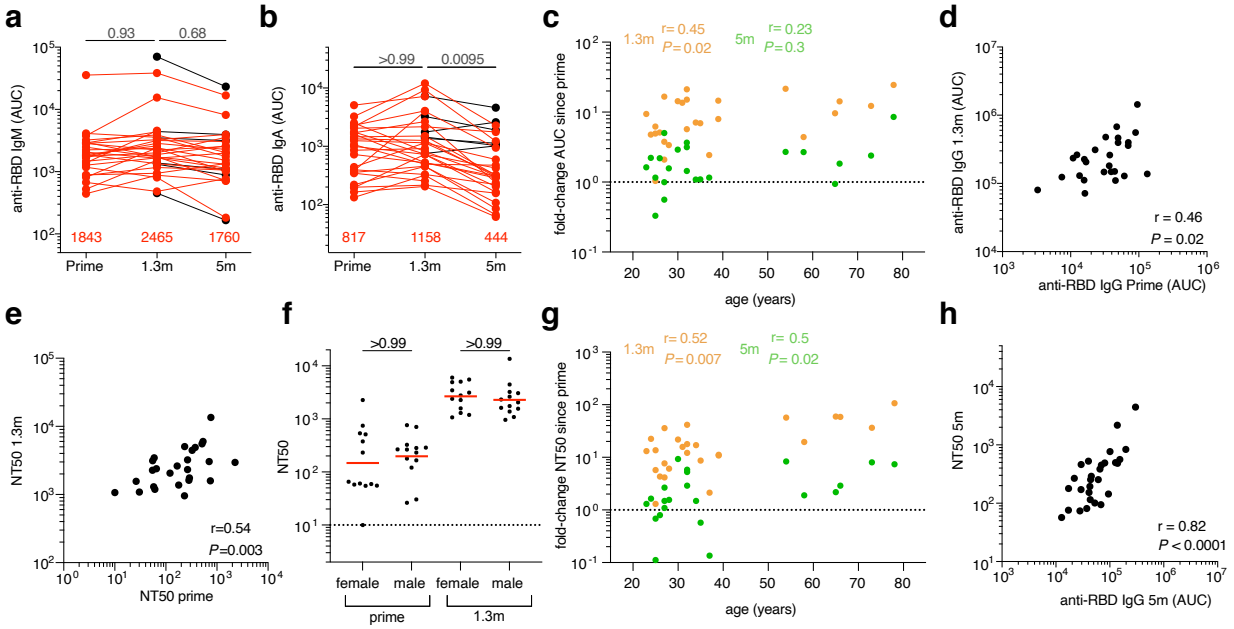

616

617 **Extended Data Fig 1: Plasma ELISA and neutralization.**

618 **a,b,** Graph shows area under the curve (AUC, Y-axis) for plasma IgM (**a**) or IgA (**b**) antibody
619 binding to SARS-CoV-2 RBD after prime, and 1.3- and 5-months post-boost for paired samples
620 from n=32 vaccinated individuals. Samples without a prime value are shown in black. **c,** Graph
621 shows age (years, X-axis) vs. fold-change of IgG-binding titers (AUC, Y-Axis) between prime
622 and 1.3m (orange) or 5m (green) post-boost. **d,** IgG antibody binding after prime (AUC, X-axis)
623 vs. IgG antibody binding after 1.3 months post-boost (AUC, Y-axis) and **e**, NT50 values after
624 prime (X-axis) vs. NT50 values after 1.3 months post-boost (Y-axis) in individuals receiving two
625 doses of an mRNA vaccine (n=26). **f,** NT50 values after prime and 1.3 months post-boost in
626 females and males receiving 2 doses of an mRNA vaccine. **g,** Graph shows age (years, X-axis) vs
627 fold-change of NT50 (X-axis) between prime and 1.3m (orange) or 5m (green) post-boost. **h,** NT50
628 values (Y-axis) vs. IgG antibody binding (AUC, X-axis) 5 months after boost in individuals

629 receiving two doses of an mRNA vaccine (n=28). All experiments were performed at least in
630 duplicate. Red values or bar in **a**, **b** and **f** represent geometric mean values. Statistical significance
631 in **a, b,** and **f** was determined by Kruskal-Wallis test with subsequent Dunn's multiple
632 comparisons, or by Spearman correlation test in **c, d, e, g,** and **h**.

633

634

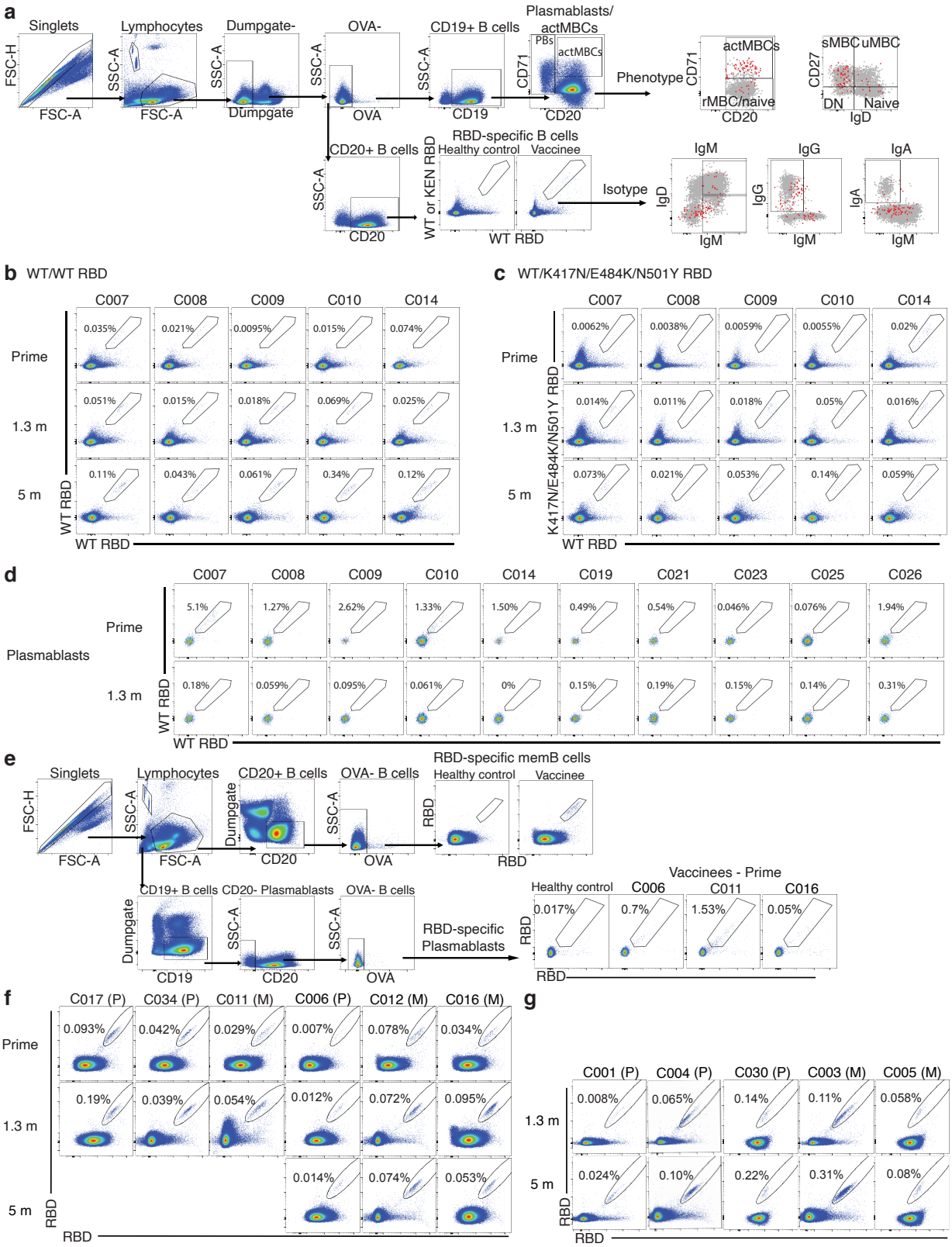
a
Singlets
Lymphocytes
Dumpgate-
OVA-
CD19+ B cells
Plasmablasts/ actMBCs
PBs
actMBCs
Phenotype
actMBCs
rMBC/naive
sMBC uMBC
DN
Naive
CD20+ B cells
RBD-specific B cells
Healthy control
Vaccinee
Isotype
IgM
IgG
IgA
b WT/WT RBD
c WT/K417N/E484K/N501Y RBD
C007 C008 C009 C010 C014
Prime
1.3 m
5 m
d
C007 C008 C009 C010 C014 C019 C021 C023 C025 C026
Plasmablasts
e
Singlets
Lymphocytes
CD20+ B cells
OVA- B cells
RBD-specific memB cells
Healthy control
Vaccinee
CD19+ B cells
CD20- Plasmablasts
OVA- B cells
RBD-specific Plasmablasts
Vaccinees - Prime
Healthy control
C006 C011 C016
f
C017 (P) C034 (P) C011 (M) C006 (P) C012 (M) C016 (M)
g
C001 (P) C004 (P) C030 (P) C003 (M) C005 (M)

635

636 **Extended Data Fig. 2: Flow Cytometry. a,** Gating strategy for phenotyping. Gating was on
637 singlets that were $CD19^+$ or $CD20^+$ and CD3-CD8-CD16-Ova-. Anti-IgG, IgM, IgA, IgD, CD71
638 and CD27 antibodies were used for B cell phenotype analysis. Antigen-specific cells were detected
639 based on binding to RBD WT-PE^+ and RBD WT/KEN (K417N/E484K/N501Y)-$AF647^+$. **b-c,**
640 Flow cytometry plots showing the frequency of **b,** RBD WT-binding memory B cells, and **c,** RBD-
641 binding memory B cells cross-reactive with WT and K417N/E484K/N501Y mutant RBD in 5
642 selected individuals, after prime, 1.3 months, and 5 months post-second vaccination. **d,** Flow
643 cytometry plots showing frequency of RBD-binding plasmablasts, in 10 selected vaccinees after
644 prime or 1.3 months post-boost. **e,** Gating strategy for single-cell sorting for CD20+ memory B
645 cells (top panel) or CD19+CD20- plasmablasts (bottom panel) which were double positive for
646 RBD-PE and RBD-AF647. **f-g,** Representative flow cytometry plots showing dual AlexaFluor-
647 647-RBD and PE-RBD-binding, single-cell sorted B cells from **f,** 6 individuals after prime and 1.3
648 months or 5 months post-boost and **g,** 5 individuals from 1.3- or 5-months post-boost. Percentage
649 of RBD-specific B cells is indicated.

650

651

652

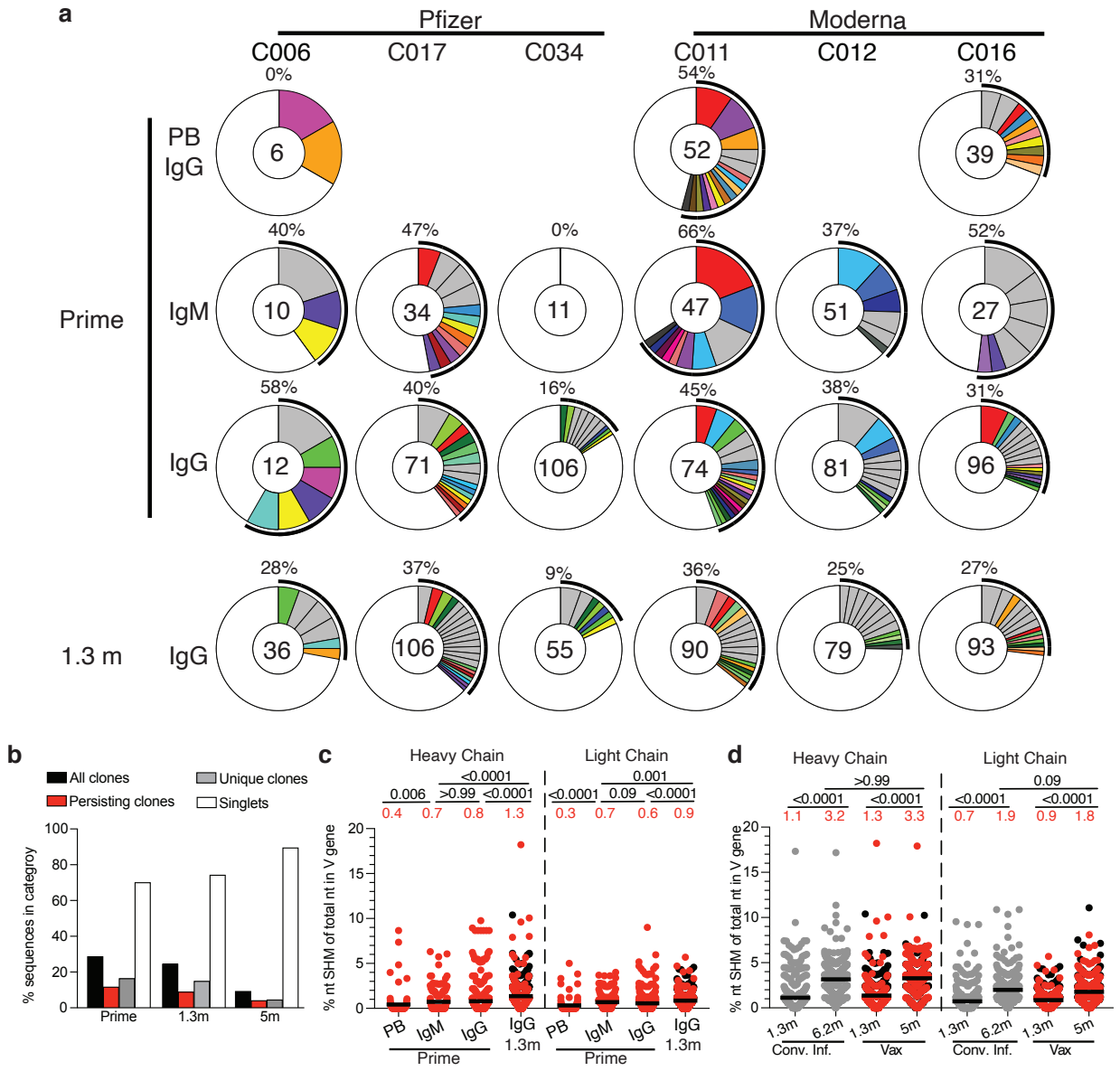

Extended Data Fig 3: anti-SARS-CoV-2 RBD-specific plasmablast and memory B cells responses after vaccination. a, Pie charts show the distribution of antibody sequences from 6 individuals after prime (upper panel) or 1.3 months post-boost (lower panel). Sequences derived from IgG plasmablast (PB), IgM memory B cells (MBC), and IgG MBC compartments were analyzed after prime, while only IgG MBCs were analyzed at 1.3 months after boost, as indicated to the left of the plots. The number inside the circle indicates the number of sequences analyzed for the individual denoted above the circle. Pie slice size is proportional to the number of clonally

661 related sequences. The black outline indicates the frequency of clonally sequences detected in each
662 patient. Colored slices indicate persisting clones (same *IGHV* and *IGLV* genes, with highly similar
663 CDR3s) found in multiple compartments and/or timepoints within the same patient. Grey slices
664 indicate clones unique to the compartment. White indicates sequences isolated once. **b,** Graph
665 shows the percentage of total paired-sequences analyzed at either prime, 1.3- or 5-months post-
666 boost, that can be found as part of all clones (black bars), persisting clones (red bars), unique clones
667 (grey bars), or singlets (white bar). **c-d,** Ratio of the number of somatic nucleotide mutations over
668 the nucleotide length of the V gene in the Ig heavy and light chains, separately, in antibodies
669 detected in **c,** different B cell compartments after prime or 1.3 months post-boost and **d,** 1.3 or 5
670 months post-boost compared to convalescent infected (grey) individuals after 1.3[3] and 6.2[7] months
671 post-infection (also Supplementary Table 4). Horizontal bars and red numbers indicate mean ratio
672 in each compartment at each time point. Sequences derived from samples without a prime value
673 are shown in black. Statistical significance in **c** and **d** was determined using a Kruskal Wallis test
674 with subsequent Dunn's multiple comparisons.
675
676

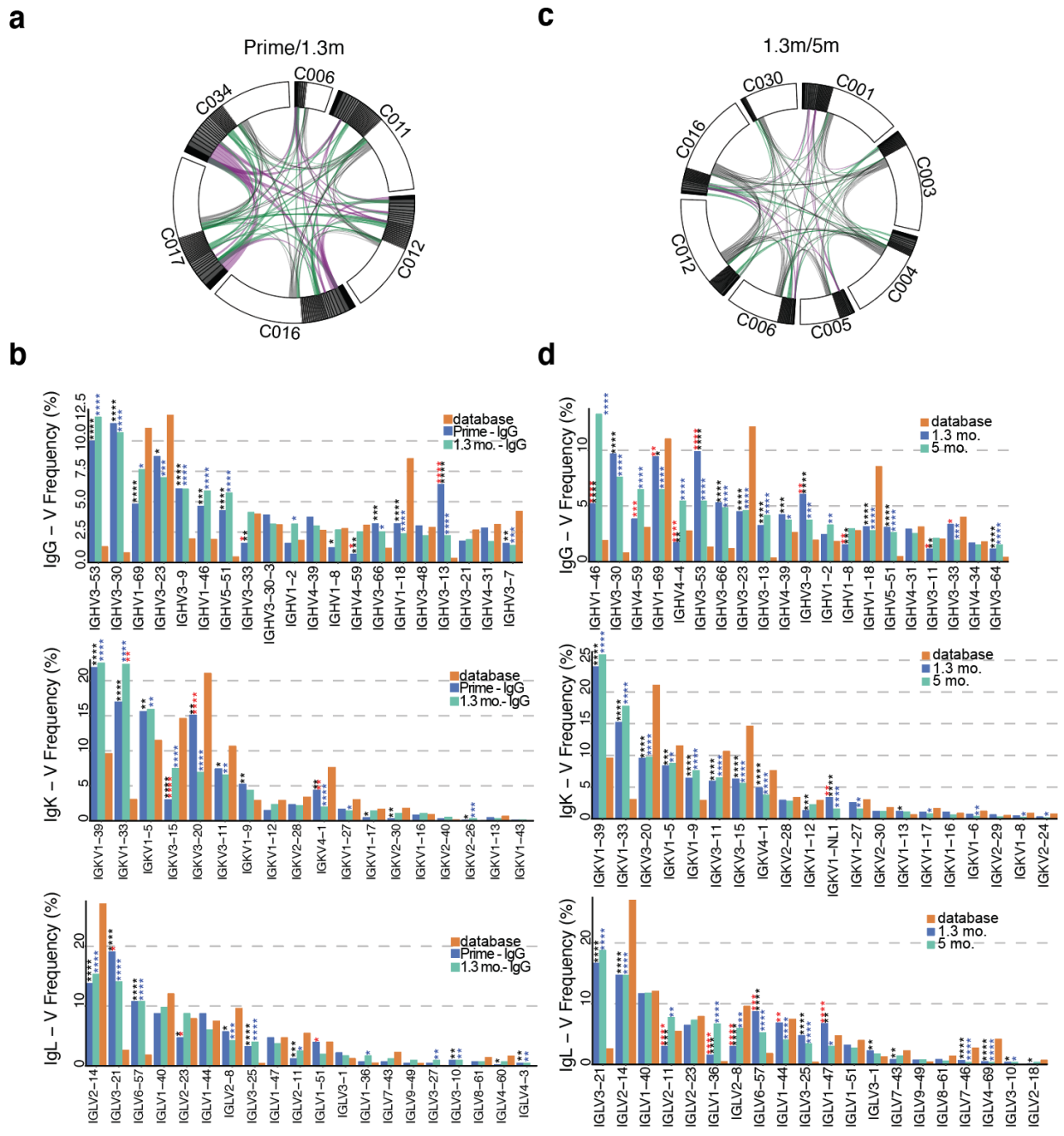

677

678 **Extended Data Fig. 4: Frequency distribution of human V genes. a,** Circos plot depicting
679 relationship between antibodies that share V and J gene usage in both IgH and IgL when comparing
680 prime/1.3m IgG MBC sequences. Purple, green, and grey lines connect related clones, clones and
681 singlets, and singlets to each other, respectively. **b,** Graph shows relative abundance of human
682 heavy chain *IGHV* (top), light chain *IGKV* (middle) or *IGLV* (bottom) genes comparing Sequence

683 Read Archive accession SRP010970 (orange), and IgG MBCs after prime (blue) or 1.3 months
684 post-boost (green). Statistical significance was determined by two-sided binomial test. * = $p \leq 0.05$,
685 ** = $p \leq 0.01$, *** = $p \leq 0.001$, **** = $p \leq 0.0001$. Color of stars indicates: black - comparing
686 Database versus Prime; blue - comparing Database versus 1.3m; red - comparing Prime versus
687 1.3m. **c,** Circos plot depicting relationship between antibodies that share V and J gene usage in
688 both IgH and IgL when comparing 1.3 m/5 m IgG MBC sequences. Purple, green, and grey lines
689 connect related clones, clones and singlets, and singlets to each other, respectively. **d,** Graph shows
690 relative abundance of human heavy chain *IGHV* (top), light chain *IGKV* (middle) or *IGLV* (bottom)
691 genes comparing Sequence Read Archive accession SRP010970 (orange), and IgG MBCs after
692 1.3 months (blue) or 5 months (green) post-vaccination. Statistical significance was determined by
693 two-sided binomial test. * = $p \leq 0.05$, ** = $p \leq 0.01$, *** = $p \leq 0.001$, **** = $p \leq 0.0001$. Color of stars
694 indicates: black - comparing Database versus 1.3 months; blue - comparing Database versus 5
695 months; red - comparing 1.3 months versus 5 months.
696
697

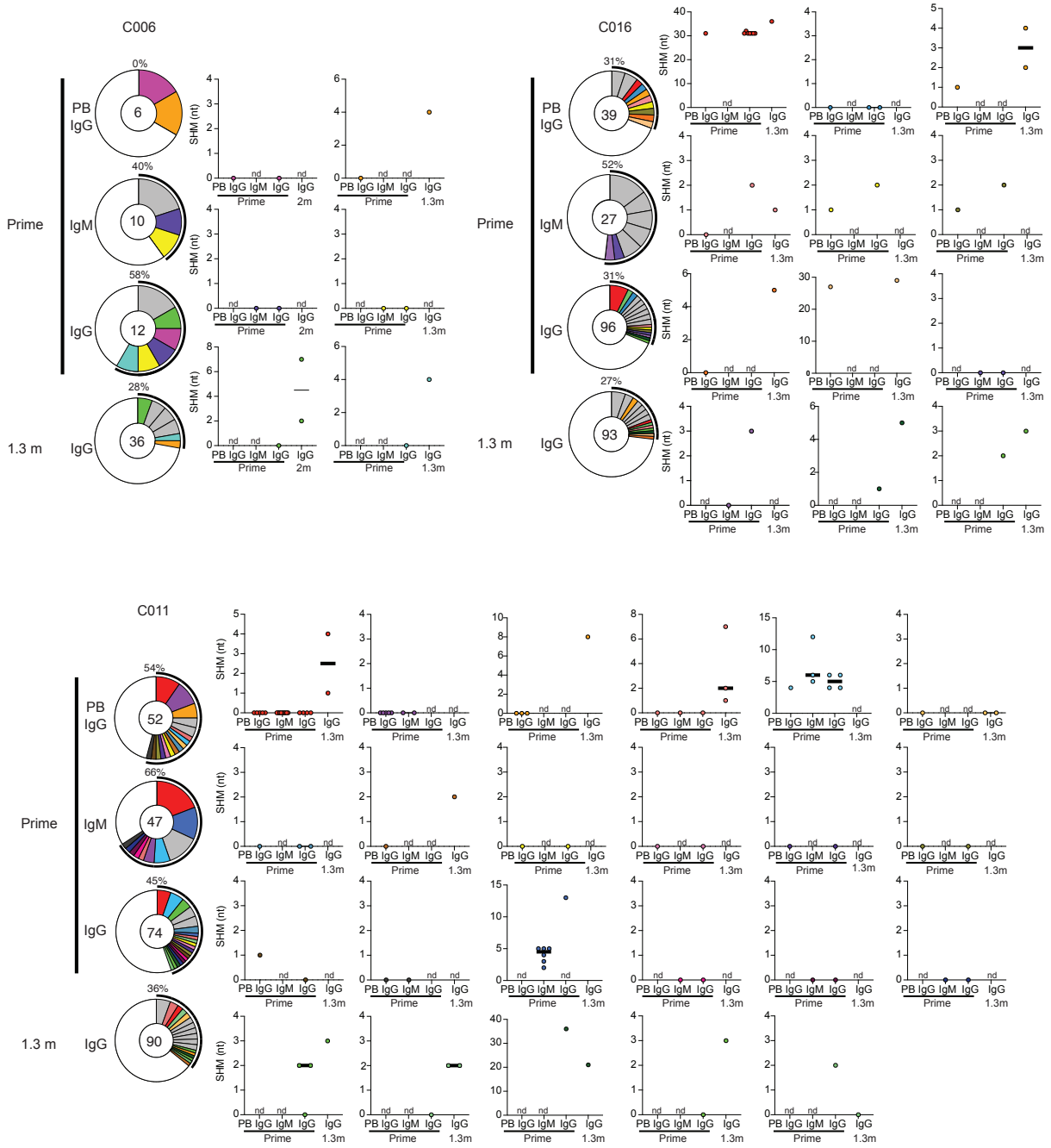

Extended Data Fig. 5: Somatic hypermutation of anti-SARS-CoV-2 RBD antibody clones after prime or boost. Clonal evolution of RBD-binding B cells from 3 individuals for which plasmablasts, IgM memory B cells, and IgG memory B cells were analyzed after prime, and IgG memory B cells were analyzed after 1.3 months post-boost (as described in Extended Data Fig. 3). The number of somatic nucleotide mutations found in shared clonal families found in at least 2

704 different compartments is graphed to the right of each donut plot. Color of dot plots match the
705 color of pie slices within the donut plot, which indicate persisting clones. nd – clone was Not
706 Detected in the indicated compartment. Black horizontal line indicates median number of SHM.
707
708

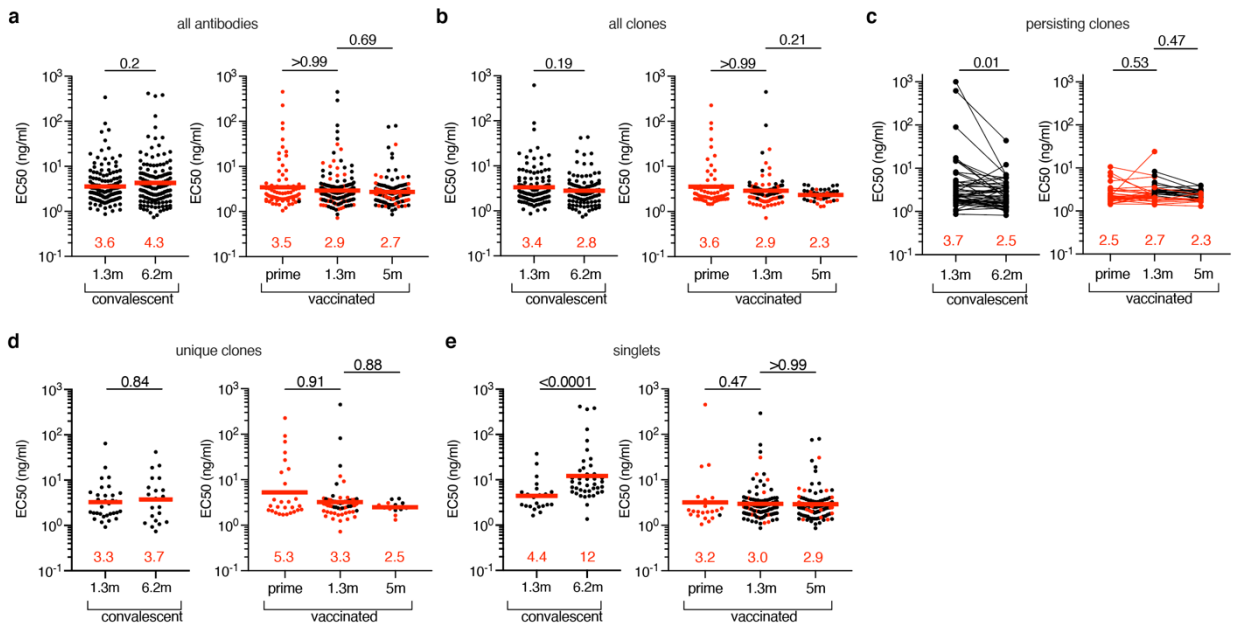

709

710 **Extended Data Fig. 6: Anti-SARS-CoV-2 RBD monoclonal antibodies ELISAs. a-e,** Graphs
711 show anti-SARS-CoV-2 binding activity of monoclonal antibodies measured by ELISA against
712 RBD. ELISA half-maximal concentration (EC_{50}) values for all antibodies (**a**), all clones (**b**),
713 persisting clones (**c**), unique clones (**d**) and singlets (**e**) isolated from COVID-19 convalescent
714 individuals 1.3[3] and 6.2[7] months after infection (left panel) or from vaccinated individuals after
715 prime, or 1.3m or 5m after receiving the second dose of mRNA vaccination (right panel). Each dot
716 represents one antibody. Antibodies isolated from samples without a prime value are shown in
717 black. Red horizontal bars and numbers indicate geometric mean values. Statistical significance
718 was determined by Mann-Whitney test (left panels of **a, b, d and e),** Kruskal-Wallis test with
719 subsequent Dunn's multiple comparisons (right panels of **a-e**) or by Wilcoxon test (left panel of
720 **c**). All experiments were performed at least twice.

721

722

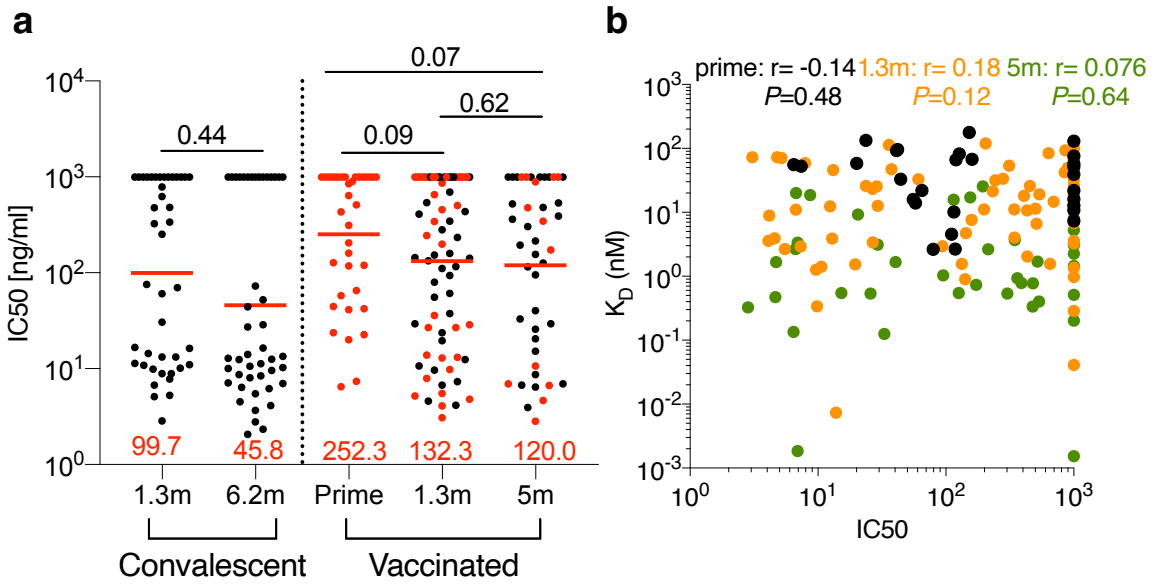

723

724 **Extended Data Fig. 7. Affinity.** Biolayer interferometry measurements. **a**, IC_{50} values for
725 randomly selected antibodies isolated from convalescents 1.3m[3] (n=42) and 6.2m[7] (n=45) after
726 infection or from vaccinees after prime (n=36), and 1.3m (n=74) and 5m (n=43). Red horizontal
727 lines and numbers indicate geometric mean. Antibodies isolated from samples without a prime
728 value are shown in black. **b,** Graphs show affinities (K_D, Y-axis) plotted against neutralization
729 activity (IC_{50}, X-axis) for antibodies isolated after prime (black), or 1.3m (orange) or 5m (green)
730 post-boost vaccination. Statistical significance was determined using Kruskal Wallis test with
731 subsequent Dunn's multiple comparisons in **a** and Spearman correlation test in **b**.

732

733

734

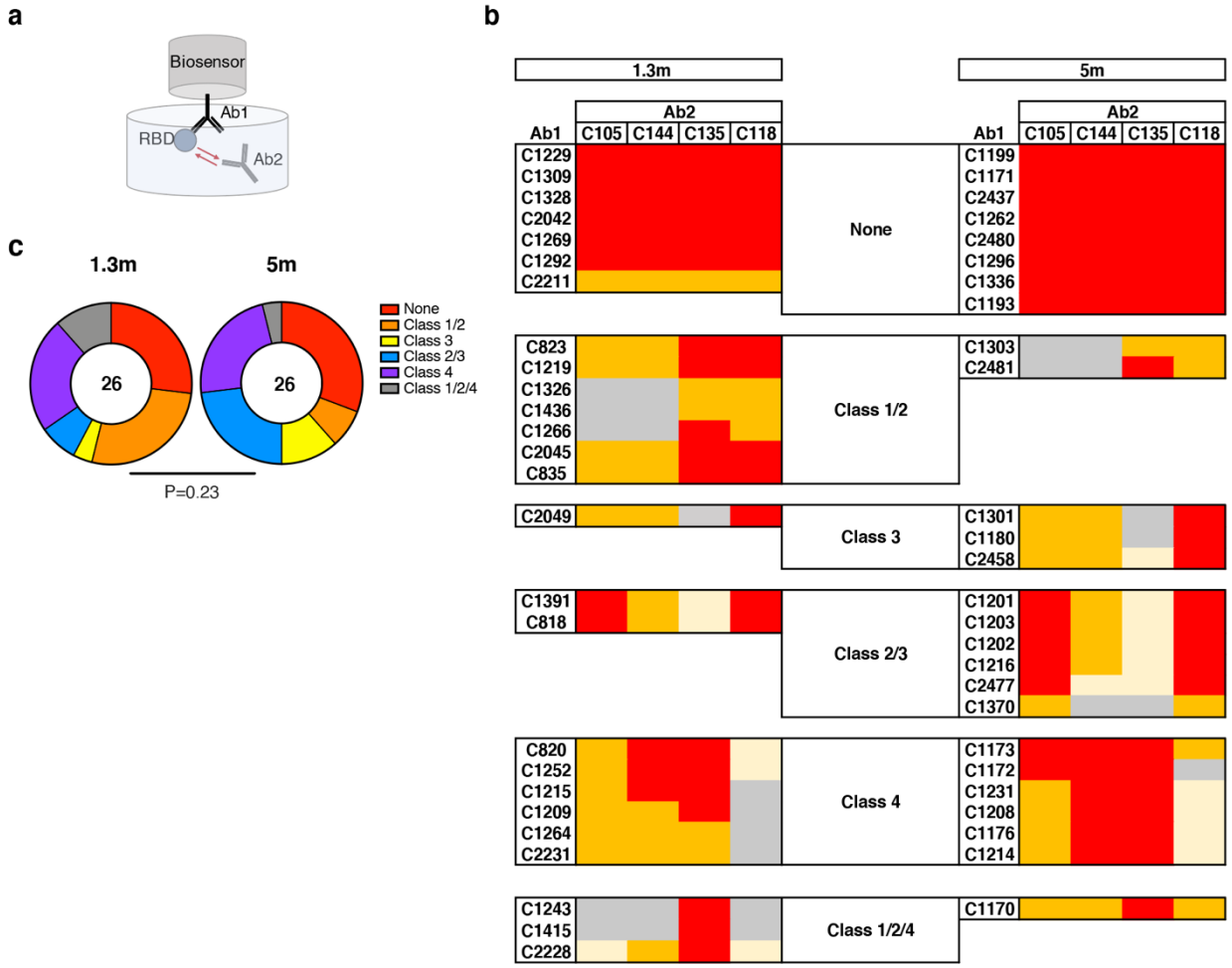

735

736 **Extended Data Fig. 8. Epitope targeting of anti-SARS-CoV-2 RBD antibodies. a**, Schematic
737 representation of the BLI experiment for randomly selected antibodies isolated from vaccinees
738 1.3- and 5 months after full vaccination (each presented group shows n=26 antibodies). **b**. Heat-
739 map of relative inhibition of Ab2 binding to the preformed Ab1-RBD complexes (grey=no
740 binding, yellow=low binding, orange=intermediate binding, red=high binding). Values are
741 normalized through the subtraction of the autologous antibody control. BLI traces can be found in
742 Extended Data Fig. 9. **c**. Pie charts indicate the fraction of antibodies that are assigned to different
743 classes according to their binding pattern as shown in **b** and Extended data Fig. 9. Number in inner

744 circle shows number of antibodies tested. Statistical significance was determined using the Chi-

745 square test in **c**.

746

747

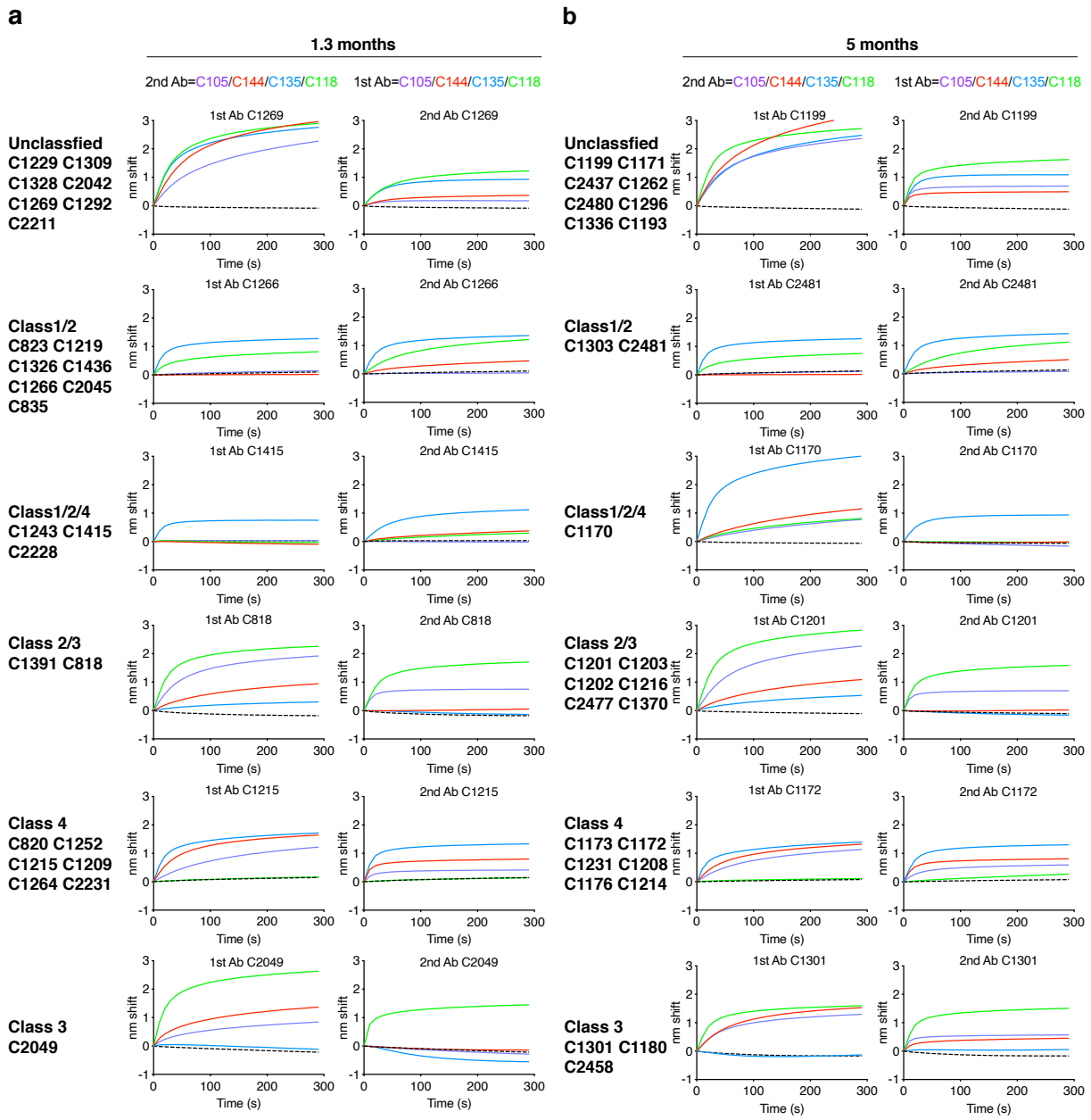

Extended Data Fig. 9. BLI traces from epitope mapping of anti-SARS-CoV-2 RBD antibodies. a-b, BLI traces from competition experiments used to determine epitope targets of anti-SARS-CoV-2 RBD antibodies isolated from vaccinees at 1.3m (**a**) or 5m (**b**) post-boost, as illustrated in Extended data Fig. 8.

a

Prime	wt	R683G	R346S	K417N	N440K	A475V	E484K R683G	Q493R	N501Y	KEN R683G	L452R E484Q R683G
C2159	12.2	6.2	9.1	3.3	11.2	8.8	627.1	17.1	20.6	212.0	36.9
C2029	25.1	7.6	>1000	5.9	23.0	19.5	1.8	14.6	57.7	1.6	>1000
C2139	46.0	25.4	33.0	>1000	48.7	>1000	153.6	>1000	>1000	>1000	105.1
C2033	46.2	25.8	32.0	>1000	41.4	868.4	79.5	183.4	668.2	>1000	52.1
C2209	52.6	26.7	40.7	12.5	48.2	214.0	107.3	341.9	214.9	58.8	44.0
C2020	65.8	37.8	164.0	>1000	53.5	71.5	131.3	>1000	119.0	>1000	83.7
C2221	69.3	26.4	47.6	>1000	58.8	>1000	355.2	>1000	46.3	>1000	124.0
C2019	88.5	96.3	>1000	25.5	90.8	70.1	726.4	92.3	125.5	380.3	>1000
C2110	118.4	106.6	92.6	>1000	109.9	797.4	254.9	198.0	301.5	>1000	218.3
C2018	118.9	37.2	55.4	33.4	110.8	98.0	284.5	123.8	135.8	140.0	>1000
C2022	153.4	61.6	114.5	>1000	130.5	>1000	247.7	358.7	162.8	>1000	139.2
C2113	348.4	127.8	242.4	166.8	267.1	347.9	>1000	922.3	339.4	>1000	>1000
C2149	376.8	178.6	259.3	>1000	331.2	>1000	724.8	>1000	>1000	>1000	608.0
C2026	433.1	25.6	258.1	400.1	350.5	925.7	188.0	368.0	387.1	190.1	147.3
C2150	591.0	57.5	672.9	496.9	413.7	783.8	240.8	406.4	543.2	202.1	199.1
C2013	593.3	204.6	391.0	>1000	484.3	117.9	>1000	>1000	>1000	>1000	>1000
C2185	670.6	116.1	440.0	239.1	494.6	818.2	412.8	759.7	485.4	246.7	251.1
C2004	722.5	117.4	529.5	521.1	468.7	>1000	400.1	496.2	928.0	318.2	345.1
C2140	840.9	124.4	706.9	839.5	778.2	>1000	648.7	866.7	815.5	481.7	497.8
C2109	1000.0	198.7	572.6	825.0	336.9	>1000	960.0	762.2	620.2	691.7	464.7

IC50 (ng/ml)

b

1.3 mo.	wt	R683G	R346S	K417N	N440K	A475V	E484K R683G	Q493R	N501Y	KEN R683G	L452R E484Q R683G
C2039	1.9	0.5	1.0	0.7	1.2	1.0	>1000	1.4	2.3	>1000	>1000
C2237	6.7	0.7	3.8	2.3	4.7	3.8	342.4	9.1	4.5	815.8	>1000
C2049	10.0	5.2	7.1	319.9	9.6	65.5	10.9	17.5	12.8	>1000	7.2
C2065	11.6	9.8	>1000	4.0	11.1	6.4	387.7	9.6	11.1	123.4	>1000
C2319	13.3	6.3	8.7	>1000	10.2	131.2	7.7	28.4	297.3	>1000	8.5
C2175	17.6	4.9	12.1	5.1	14.2	8.0	506.1	>1000	17.5	347.0	23.5
C2219	20.7	9.8	13.0	5.2	19.4	35.1	>1000	369.6	13.7	>1000	>1000
C2227	48.3	28.5	94.8	20.6	45.0	36.8	>1000	8.7	>1000	>1000	14.3
C2047	49.1	40.4	145.2	>1000	48.8	53.2	168.6	>1000	96.8	>1000	123.4
C2045	52.0	41.2	46.4	>1000	61.1	375.8	62.9	>1000	60.3	>1000	76.4
C2188	90.8	45.7	64.3	>1000	56.6	743.4	134.8	>1000	>1000	>1000	119.6
C2037	148.1	74.1	53.1	32.7	88.0	103.4	378.3	147.5	157.4	246.4	>1000
C2228	178.4	145.9	124.1	70.2	132.2	>1000	770.5	>1000	197.9	886.3	785.3
C2167	200.4	140.1	156.4	13.6	144.2	143.0	287.9	233.5	183.3	28.4	243.6
C2318	351.9	126.5	262.1	113.7	241.7	335.9	286.4	311.0	477.8	244.8	231.4
C2210	366.2	145.7	236.9	188.6	270.5	297.1	382.6	333.2	276.1	381.7	363.0
C2317	429.2	549.9	>1000	105.5	296.6	282.1	>1000	305.6	387.5	>1000	>1000
C2172	451.6	246.0	324.0	214.0	257.3	>1000	363.5	>1000	486.9	>1000	199.7
C2070	584.0	532.7	856.2	260.7	529.0	709.6	884.3	629.7	802.5	838.8	578.2
C2321	843.9	254.3	>1000	648.9	>1000	627.1	400.1	316.5	693.4	445.2	>1000

IC50 (ng/ml)

Extended Data Fig. 10: Breadth of anti-SARS-CoV-2 RBD antibodies elicited after prime and 2 doses of vaccination. **a-b**, IC_{50} values for n=40 neutralizing antibodies isolated after prime **(a)** or 1.3 months post-boost **(b)** against indicated mutant SARS-CoV-2 pseudoviruses. Color gradient indicates IC_{50} values ranging from 0 (white) to 1000 ng/ml (red).

761 **REFERENCES**

762 1 Wang, Z. *et al.* Naturally enhanced neutralizing breadth against SARS-CoV-2 one year
763 after infection. *Nature*, doi:10.1038/s41586-021-03696-9 (2021).
764 2 Goel, R. R. *et al.* Distinct antibody and memory B cell responses in SARS-CoV-2 naive and
765 recovered individuals following mRNA vaccination. *Sci Immunol* **6**,
766 doi:10.1126/sciimmunol.abi6950 (2021).
767 3 Robbiani, D. F. *et al.* Convergent antibody responses to SARS-CoV-2 in convalescent
768 individuals. *Nature* **584**, 437-442, doi:10.1038/s41586-020-2456-9 (2020).
769 4 Apostolidis, S. A. *et al.* Altered cellular and humoral immune responses following SARS-
770 CoV-2 mRNA vaccination in patients with multiple sclerosis on anti-CD20 therapy.
771 *medRxiv*, 2021.2006.2023.21259389, doi:10.1101/2021.06.23.21259389 (2021).
772 5 Sokal, A. *et al.* Memory B cells control SARS-CoV-2 variants upon mRNA vaccination of
773 naive and COVID-19 recovered individuals. *bioRxiv*, 2021.2006.2017.448459,
774 doi:10.1101/2021.06.17.448459 (2021).
775 6 Turner, J. S. *et al.* SARS-CoV-2 mRNA vaccines induce persistent human germinal centre
776 responses. *Nature*, doi:10.1038/s41586-021-03738-2 (2021).
777 7 Gaebler, C. *et al.* Evolution of antibody immunity to SARS-CoV-2. *Nature* **591**, 639-644,
778 doi:10.1038/s41586-021-03207-w (2021).
779 8 Schmidt, F. *et al.* Measuring SARS-CoV-2 neutralizing antibody activity using
780 pseudotyped and chimeric viruses. *J Exp Med* **217**, doi:10.1084/jem.20201181 (2020).
781 9 Pilishvili, T. *et al.* Interim Estimates of Vaccine Effectiveness of Pfizer-BioNTech and
782 Moderna COVID-19 Vaccines Among Health Care Personnel - 33 U.S. Sites, January-
783 March 2021. *MMWR Morb Mortal Wkly Rep* **70**, 753-758,
784 doi:10.15585/mmwr.mm7020e2 (2021).
785 10 Lopez Bernal, J. *et al.* Effectiveness of Covid-19 Vaccines against the B.1.617.2 (Delta)
786 Variant. *N Engl J Med*, doi:10.1056/NEJMoa2108891 (2021).
787 11 Amanat, F. *et al.* SARS-CoV-2 mRNA vaccination induces functionally diverse antibodies
788 to NTD, RBD, and S2. *Cell* **184**, 3936-3948 e3910, doi:10.1016/j.cell.2021.06.005 (2021).
789 12 Reynolds, C. J. *et al.* Prior SARS-CoV-2 infection rescues B and T cell responses to
790 variants after first vaccine dose. *Science*, doi:10.1126/science.abh1282 (2021).
791 13 Wang, Z. *et al.* mRNA vaccine-elicited antibodies to SARS-CoV-2 and circulating variants.
792 *Nature* **592**, 616-622, doi:10.1038/s41586-021-03324-6 (2021).
793 14 Stamatatos, L. *et al.* mRNA vaccination boosts cross-variant neutralizing antibodies
794 elicited by SARS-CoV-2 infection. *Science*, doi:10.1126/science.abg9175 (2021).
795 15 West, A. P. *et al.* Detection and characterization of the SARS-CoV-2 lineage B.1.526 in
796 New York. *bioRxiv*, doi:10.1101/2021.02.14.431043 (2021).
797 16 Edara, V. V. *et al.* Infection and Vaccine-Induced Neutralizing-Antibody Responses to the
798 SARS-CoV-2 B.1.617 Variants. *N Engl J Med*, doi:10.1056/NEJMc2107799 (2021).
799 17 Planas, D. *et al.* Reduced sensitivity of SARS-CoV-2 variant Delta to antibody
800 neutralization. *Nature*, doi:10.1038/s41586-021-03777-9 (2021).
801 18 Victora, G. D. & Nussenzweig, M. C. Germinal centers. *Annu Rev Immunol* **30**, 429-457,
802 doi:10.1146/annurev-immunol-020711-075032 (2012).

803 19 Dugan, H. L. *et al.* Profiling B cell immunodominance after SARS-CoV-2 infection reveals
804 antibody evolution to non-neutralizing viral targets. *Immunity* **54**, 1290-1303 e1297,
805 doi:10.1016/j.immuni.2021.05.001 (2021).
806 20 Li, D. *et al.* In vitro and in vivo functions of SARS-CoV-2 infection-enhancing and
807 neutralizing antibodies. *Cell* **184**, 4203-4219 e4232, doi:10.1016/j.cell.2021.06.021
808 (2021).
809 21 Brouwer, P. J. M. *et al.* Potent neutralizing antibodies from COVID-19 patients define
810 multiple targets of vulnerability. *Science* **369**, 643-650, doi:10.1126/science.abc5902
811 (2020).
812 22 Kreer, C. *et al.* Longitudinal Isolation of Potent Near-Germline SARS-CoV-2-Neutralizing
813 Antibodies from COVID-19 Patients. *Cell* **182**, 843-854 e812,
814 doi:10.1016/j.cell.2020.06.044 (2020).
815 23 Seydoux, E. *et al.* Analysis of a SARS-CoV-2-Infected Individual Reveals Development of
816 Potent Neutralizing Antibodies with Limited Somatic Mutation. *Immunity* **53**, 98-105
817 e105, doi:10.1016/j.immuni.2020.06.001 (2020).
818 24 Taylor, J. J., Pape, K. A., Steach, H. R. & Jenkins, M. K. Humoral immunity. Apoptosis and
819 antigen affinity limit effector cell differentiation of a single naive B cell. *Science* **347**,
820 784-787, doi:10.1126/science.aaa1342 (2015).
821 25 Muecksch, F. *et al.* Affinity maturation of SARS-CoV-2 neutralizing antibodies confers
822 potency, breadth, and resilience to viral escape mutations. *Immunity* **54**, 1853-1868
823 e1857, doi:10.1016/j.immuni.2021.07.008 (2021).
824 26 Li, G. M. *et al.* Pandemic H1N1 influenza vaccine induces a recall response in humans
825 that favors broadly cross-reactive memory B cells. *Proc Natl Acad Sci U S A* **109**, 9047-
826 9052, doi:10.1073/pnas.1118979109 (2012).
827 27 Wrammert, J. *et al.* Rapid and massive virus-specific plasmablast responses during acute
828 dengue virus infection in humans. *J Virol* **86**, 2911-2918, doi:10.1128/JVI.06075-11
829 (2012).
830 28 Wrammert, J. *et al.* Rapid cloning of high-affinity human monoclonal antibodies against
831 influenza virus. *Nature* **453**, 667-671, doi:10.1038/nature06890 (2008).
832 29 Amanna, I. J., Carlson, N. E. & Slifka, M. K. Duration of humoral immunity to common
833 viral and vaccine antigens. *N Engl J Med* **357**, 1903-1915, doi:10.1056/NEJMoa066092
834 (2007).
835 30 Davis, C. W. *et al.* Influenza vaccine-induced human bone marrow plasma cells decline
836 within a year after vaccination. *Science* **370**, 237-241, doi:10.1126/science.aaz8432
837 (2020).
838 31 Halliley, J. L. *et al.* Long-Lived Plasma Cells Are Contained within the CD19(-
839)CD38(hi)CD138(+) Subset in Human Bone Marrow. *Immunity* **43**, 132-145,
840 doi:10.1016/j.immuni.2015.06.016 (2015).
841 32 Slifka, M. K., Antia, R., Whitmire, J. K. & Ahmed, R. Humoral immunity due to long-lived
842 plasma cells. *Immunity* **8**, 363-372, doi:10.1016/s1074-7613(00)80541-5 (1998).
843 33 Dan, J. M. *et al.* Immunological memory to SARS-CoV-2 assessed for up to 8 months
844 after infection. *Science* **371**, doi:10.1126/science.abf4063 (2021).
845 34 Sakharkar, M. *et al.* Prolonged evolution of the human B cell response to SARS-CoV-2
846 infection. *Sci Immunol* **6**, doi:10.1126/sciimmunol.abg6916 (2021).

847 35 Widge, A. T. *et al.* Durability of Responses after SARS-CoV-2 mRNA-1273 Vaccination. *N*
848 *Engl J Med* **384**, 80-82, doi:10.1056/NEJMc2032195 (2021).
849 36 Wajnberg, A. *et al.* Robust neutralizing antibodies to SARS-CoV-2 infection persist for
850 months. *Science* **370**, 1227-1230, doi:10.1126/science.abd7728 (2020).
851 37 Pegu, A. *et al.* Durability of mRNA-1273-induced antibodies against SARS-CoV-2 variants.
852 *bioRxiv*, doi:10.1101/2021.05.13.444010 (2021).
853 38 Chen, R. E. *et al.* Resistance of SARS-CoV-2 variants to neutralization by monoclonal and
854 serum-derived polyclonal antibodies. *Nat Med* **27**, 717-726, doi:10.1038/s41591-021-
855 01294-w (2021).
856 39 Abu-Raddad, L. J., Chemaitelly, H., Butt, A. A. & National Study Group for, C.-V.
857 Effectiveness of the BNT162b2 Covid-19 Vaccine against the B.1.1.7 and B.1.351
858 Variants. *N Engl J Med* **385**, 187-189, doi:10.1056/NEJMc2104974 (2021).
859 40 Hacisuleyman, E. *et al.* Vaccine Breakthrough Infections with SARS-CoV-2 Variants. *N*
860 *Engl J Med* **384**, 2212-2218, doi:10.1056/NEJMoa2105000 (2021).
861 41 Lumley, S. F. *et al.* Antibody Status and Incidence of SARS-CoV-2 Infection in Health Care
862 Workers. *N Engl J Med* **384**, 533-540, doi:10.1056/NEJMoa2034545 (2021).
863 42 Gazit, S. *et al.* Comparing SARS-CoV-2 natural immunity to vaccine-induced immunity:
864 reinfections versus breakthrough infections. *medRxiv*, 2021.2008.2024.21262415,
865 doi:10.1101/2021.08.24.21262415 (2021).
866 43 McHeyzer-Williams, L. J., Milpied, P. J., Okitsu, S. L. & McHeyzer-Williams, M. G. Class-
867 switched memory B cells remodel BCRs within secondary germinal centers. *Nat Immunol*
868 **16**, 296-305, doi:10.1038/ni.3095 (2015).
869 44 Mesin, L. *et al.* Restricted Clonality and Limited Germinal Center Reentry Characterize
870 Memory B Cell Reactivation by Boosting. *Cell* **180**, 92-106 e111,
871 doi:10.1016/j.cell.2019.11.032 (2020).
872 45 Pape, K. A., Taylor, J. J., Maul, R. W., Gearhart, P. J. & Jenkins, M. K. Different B cell
873 populations mediate early and late memory during an endogenous immune response.
874 *Science* **331**, 1203-1207, doi:10.1126/science.1201730 (2011).
875 46 Viant, C. *et al.* Antibody Affinity Shapes the Choice between Memory and Germinal
876 Center B Cell Fates. *Cell* **183**, 1298-1311 e1211, doi:10.1016/j.cell.2020.09.063 (2020).
877 47 Sokal, A. *et al.* Maturation and persistence of the anti-SARS-CoV-2 memory B cell
878 response. *Cell* **184**, 1201-1213 e1214, doi:10.1016/j.cell.2021.01.050 (2021).
879 48 Feng, L. *et al.* An adenovirus-vectored COVID-19 vaccine confers protection from SARS-
880 COV-2 challenge in rhesus macaques. *Nat Commun* **11**, 4207, doi:10.1038/s41467-020-
881 18077-5 (2020).
882 49 Hassan, A. O. *et al.* A Single-Dose Intranasal ChAd Vaccine Protects Upper and Lower
883 Respiratory Tracts against SARS-CoV-2. *Cell* **183**, 169-184 e113,
884 doi:10.1016/j.cell.2020.08.026 (2020).
885 50 Greaney, A. J. *et al.* Antibodies elicited by mRNA-1273 vaccination bind more broadly to
886 the receptor binding domain than do those from SARS-CoV-2 infection. *Sci Transl Med*
887 **13**, doi:10.1126/scitranslmed.abi9915 (2021).
888 51 Pardi, N. *et al.* Expression kinetics of nucleoside-modified mRNA delivered in lipid
889 nanoparticles to mice by various routes. *J Control Release* **217**, 345-351,
890 doi:10.1016/j.jconrel.2015.08.007 (2015).

891 52 Wu, K. *et al.* Preliminary Analysis of Safety and Immunogenicity of a SARS-CoV-2 Variant
892 Vaccine Booster. *medRxiv*, 2021.2005.2005.21256716,
893 doi:10.1101/2021.05.05.21256716 (2021).
894 53 Khoury, D. S. *et al.* Neutralizing antibody levels are highly predictive of immune
895 protection from symptomatic SARS-CoV-2 infection. *Nat Med* **27**, 1205-1211,
896 doi:10.1038/s41591-021-01377-8 (2021).
897 54 Wu, F. *et al.* A new coronavirus associated with human respiratory disease in China.
898 *Nature* **579**, 265-269, doi:10.1038/s41586-020-2008-3 (2020).
899 55 Amanat, F. *et al.* A serological assay to detect SARS-CoV-2 seroconversion in humans.
900 *Nat Med* **26**, 1033-1036, doi:10.1038/s41591-020-0913-5 (2020).
901 56 Grifoni, A. *et al.* Targets of T Cell Responses to SARS-CoV-2 Coronavirus in Humans with
902 COVID-19 Disease and Unexposed Individuals. *Cell* **181**, 1489-1501 e1415,
903 doi:10.1016/j.cell.2020.05.015 (2020).
904 57 Barnes, C. O. *et al.* Structures of Human Antibodies Bound to SARS-CoV-2 Spike Reveal
905 Common Epitopes and Recurrent Features of Antibodies. *Cell* **182**, 828-842 e816,
906 doi:10.1016/j.cell.2020.06.025 (2020).
907 58 Weisblum, Y. *et al.* Escape from neutralizing antibodies by SARS-CoV-2 spike protein
908 variants. *Elife* **9**, doi:10.7554/eLife.61312 (2020).
909 59 Wang, Z. *et al.* Enhanced SARS-CoV-2 neutralization by dimeric IgA. *Sci Transl Med* **13**,
910 doi:10.1126/scitranslmed.abf1555 (2021).
911 60 Gupta, N. T. *et al.* Change-O: a toolkit for analyzing large-scale B cell immunoglobulin
912 repertoire sequencing data. *Bioinformatics* **31**, 3356-3358,
913 doi:10.1093/bioinformatics/btv359 (2015).
914 61 Soto, C. *et al.* High frequency of shared clonotypes in human B cell receptor repertoires.
915 *Nature* **566**, 398-402, doi:10.1038/s41586-019-0934-8 (2019).
916 62 Guo, Y., Chen, K., Kwong, P. D., Shapiro, L. & Sheng, Z. cAb-Rep: A Database of Curated
917 Antibody Repertoires for Exploring Antibody Diversity and Predicting Antibody
918 Prevalence. *Front Immunol* **10**, 2365, doi:10.3389/fimmu.2019.02365 (2019).
919